

## Low-dimensional trapped gases

D. S. Petrov<sup>1,2</sup>, D. M. Gangardt<sup>3</sup> and G. V. Shlyapnikov<sup>1,2,3</sup><sup>1</sup> FOM Institute AMOLF, Kruislaan 407, 1098 SJ Amsterdam, The Netherlands<sup>2</sup> Russian Research Center Kurchatov Institute, Kurchatov Square, 123182 Moscow, Russia<sup>3</sup> Laboratoire Kastler Brossel, Ecole Normale Supérieure, 24 rue Lhomond, 75231, Paris, France

## Abstract

Recent developments in the physics of ultracold gases provide wide possibilities for reducing the dimensionality of space for magnetically or optically trapped atoms. The goal of these lectures is to show that regimes of quantum degeneracy in two-dimensional (2D) and one-dimensional (1D) trapped gases are drastically different from those in three dimensions and to stimulate an interest in low-dimensional systems. Attention is focused on the new physics appearing in currently studied low-dimensional trapped gases and related to finite-size and finite-temperature effects.

## Contents

1	Lecture 1. BEC in ideal 2D and 1D gases	2
1.1	Uniform ideal gas	3
1.2	Ideal gas in a harmonic trap	3
2	Lecture 2. Interactions and BEC regimes in 2D trapped gases	6
2.1	Weakly interacting regime	7
2.2	Quasi-2D scattering problem	9
2.3	True BEC at $T = 0$	12
2.4	Quasicondensate at finite temperatures	14
2.5	True and quasicondensates in 2D traps	17
3	Lecture 3. True and quasicondensates in 1D trapped gases	20
3.1	Weakly interacting regime in 1D	21
3.2	True BEC and diagram of states at $T = 0$	22
3.3	Regimes of quantum degeneracy at finite temperature	23
3.4	Phase coherence in 3D elongated condensates	27

Present address: ITAMP, Harvard-Smithsonian Center for Astrophysics, and Harvard-MIT Center for Ultracold Atoms, Department of Physics, Cambridge, Massachusetts 02138, USA

Present address: Laboratoire de Physique Théorique et Modèles Statistiques, Université Paris Sud, 91405, Orsay Cedex, France, and Van der Waals-Zeeman Institute, University of Amsterdam, Valckenierstraat 65/67, 1018 XE Amsterdam, The Netherlands

4	Lecture 4. Correlations in strongly interacting 1D Bose gases	30
4.1	Lieb-Liniger model for trapped 1D gases	30
4.2	Phase coherence at zero temperature	32
4.3	Local correlations at $T = 0$	34
4.4	Finite-temperature local correlations	38
4.5	Acknowledgements	40

## INTRODUCTION

The subject of low-dimensional quantum gases has a long pre-history. The influence of dimensionality of the system of bosons on the presence and character of Bose-Einstein condensation (BEC) and superfluid phase transition has been a subject of extensive studies in the spatially homogeneous case. From a general point of view, the absence of a true condensate in 2D and 1D at finite temperatures follows from the Bogoliubov  $k^{-2}$  theorem and originates from long-wave fluctuations of the phase (see, e.g., [1]). This has been expounded by Mermin and Wagner [2] and by Hohenberg [3], and formed a basis for later investigations.

The earlier discussion of low-dimensional Bose gases was mostly academic as there was no possible realization of such a system. Fast progress in evaporative and optical cooling of trapped atoms and the observation of Bose-Einstein condensation (BEC) in trapped clouds of alkali atoms [4-6] stimulated a search for non-trivial trapping geometries. Present facilities allow one to tightly confine the motion of trapped particles in one (two) direction(s) to zero point oscillations. Then, kinematically the gas is 2D (1D), and the difference from purely 2D (1D) gases is only related to the value of the effective interparticle interaction which now depends on the tight confinement.

Recent experiments have already reached 2D and 1D regimes for trapped Bose gases and studied some of the quantum degenerate states. These studies bring in new physics originating from a finite size of the system, spatial inhomogeneity, and finite temperatures. The present lectures cover most important issues in the physics of 2D and 1D trapped quantum gases: the nature of various quantum degenerate states, the role of interaction between particles, and the role of finite-temperature and finite-size effects.

## 1 LECTURE 1. BEC IN IDEAL 2D AND 1D GASES

We start with describing a cross-over to the BEC regime in ideal 2D and 1D Bose gases with a finite number of particles. We will consider an equilibrium gas at temperature  $T$  in the grand canonical ensemble, where the chemical potential is fixed and the number of particles  $N$  is fluctuating. In the thermodynamic limit ( $N \rightarrow \infty$ ) this is equivalent to the description in the canonical ensemble (fixed  $N$  and fluctuating  $\mu$ ).

In any dimension and confining potential the gas is characterized by a set of eigenenergies of an individual particle,  $E_i$ , with the index  $i$  labeling quantum numbers of the particle eigenstates. The (average) total number of particles  $N$  is then related to the temperature and chemical potential by the equation

$$N = \sum_i N_i \frac{e^{-\beta E_i}}{1 - e^{-\beta E_i}}; \quad (1.1)$$

where  $N_i(z) = 1/(e^{\beta E_i} - 1)$  are the equilibrium occupation numbers of the eigenstates. We now demonstrate how Eq.(1.1) allows one to establish the presence or absence of BEC in 2D and 1D ideal Bose gases.

### 1.1 Uniform ideal gas

In an infinitely large uniform gas the particle eigenstates are characterized by the momentum  $\mathbf{k}$  and the eigenenergy  $E_{\mathbf{k}} = \hbar^2 \mathbf{k}^2 / 2m$ , where  $m$  is the mass of a particle. Then Eq.(1.1) takes the form

$$N = \int \frac{d^d \mathbf{k}}{(2\pi)^d} N_{\mathbf{k}} \frac{E_{\mathbf{k}}}{T} ; \quad (1.2)$$

with  $d$  being the dimension of the system, and  $V$  the  $d$ -dimensional volume.

In the 2D case the integration in Eq.(1.2) is straightforward and we obtain

$$\mu = T \ln \left[ 1 - \exp \left( - \frac{\hbar^2}{2mT} \right) \right] < 0 ; \quad (1.3)$$

where  $\lambda_T = (2\pi\hbar^2/mT)^{1/2}$  is the thermal de Broglie wavelength, and  $n_2$  is the 2D density. The quantity  $n_2 \lambda_T^2$  is called the degeneracy parameter and in 2D it can be written as  $n_2 \lambda_T^2 = T/T_d$ , where  $T_d = \hbar^2 n_2 / m$  is the temperature of quantum degeneracy. In the limit of a classical gas,  $n_2 \lambda_T^2 \ll 1$ , Eq.(1.3) gives the well-known result  $\mu = T \ln(n_2 \lambda_T^2)$ . For a strongly degenerate gas, where  $n_2 \lambda_T^2 \gg 1$ , we obtain  $\mu = T \exp(-\hbar^2/2mT)$ . Unlike in the 3D case, the dependence  $\mu(T)$  is analytical and it shows a monotonic increase of the chemical potential with decreasing temperature up to  $T \rightarrow 0$ . In the thermodynamic limit the population of the ground state ( $\mathbf{k} = 0$ ) remains microscopic. One thus can say that there is no BEC in a finite-temperature ideal uniform 2D Bose gas.

The situation is similar for an infinite uniform 1D Bose gas, where the degeneracy parameter is  $n_1 \lambda_T = (T/T_d)^{1/2}$  and the temperature of quantum degeneracy is given by  $T_d = \hbar^2 n_1^2 / m$ , with  $n_1$  being the 1D density. In the classical limit ( $n_1 \lambda_T \ll 1$ ), and in the limit of a strongly degenerate gas ( $n_1 \lambda_T \gg 1$ ), Eq.(1.2) gives

$$\mu = T \ln(n_1 \lambda_T) ; \quad n_1 \lambda_T \ll 1 ; \quad (1.4)$$

$$\mu = \frac{T}{(n_1 \lambda_T)^2} ; \quad n_1 \lambda_T \gg 1 ; \quad (1.5)$$

Again, the chemical potential monotonically decreases with temperature and remains negative at any  $T$ , which indicates the absence of BEC.

The absence of BEC in infinitely large uniform 2D and 1D Bose gases is a striking difference from the 3D case. This difference originates from the energy dependence of the density of states. The (energy) density of states is  $\rho(E) \propto E^{(d-1)/2}$ , where  $d$  is the dimension of the system, and for the 3D gas it decreases with  $E$ . Therefore, at sufficiently low temperatures it becomes impossible to thermally occupy the low energy states while maintaining a constant chemical potential or density. As a result, a macroscopic number of particles goes to the ground state ( $\mathbf{k} = 0$ ), i.e. one has the phenomenon of BEC. In 2D and 1D the density of states does not decrease with  $E$  and this phenomenon is absent.

### 1.2 Ideal gas in a harmonic trap

For 2D and 1D Bose gases in a harmonic confining potential the density of states is  $\rho(E) \propto E^{(d-1)}$  and the situation changes. The population of the ground state ( $E = 0$ ) is

$$N_0 = \frac{1}{\exp(\mu/T) + 1} ; \quad (1.6)$$

For a large but finite number of particles in a trap,  $N_0$  can become macroscopic (comparable with  $N$ ) at a small but finite negative  $\mu$ . One then speaks of a cross-over to the BEC regime.

We first discuss the BEC cross-over for the 2D Bose gas in a symmetric harmonic confining potential  $V(r) = m\omega^2(x^2 + y^2)/2$ . In this case the particle energy is  $E = \hbar\omega(n_x + n_y)$ , with quantum numbers  $n_x, n_y$  being non-negative integers. The density of states is then  $\rho(E) = E/(\hbar\omega)^2$ , and the contribution of low-energy excited states to the total number of particles is negligible. Therefore, separating out the population of the ground state, one can replace the summation in Eq.(1.1) by integration:

$$N = N_0 + \int_0^\infty dE \rho(E) N \frac{E}{T} \quad (1.7)$$

Assuming a large population of the ground state, from Eq.(1.6) we obtain  $T = T_c(1 - N_0/N)^{-1}$ , and the population of excited trap states proves to be

$$\int_0^\infty dE \rho(E) N \frac{E}{T} = \frac{T}{\hbar\omega} \frac{2}{6} \frac{1 + \ln N_0}{N_0} \quad (1.8)$$

This allows us to write Eq.(1.7) in the form

$$N - 1 = \frac{T}{T_c} \frac{2}{6} \frac{1 + \ln N_0}{N_0} \quad (1.9)$$

where

$$T_c = \frac{\hbar\omega}{2} \frac{6N}{\ln N} \quad (1.10)$$

For a large number of particles, Eq. (1.9) indicates the presence of a sharp cross-over to the BEC regime at  $T = T_c$ . Below  $T_c$  we omit the last term in Eq.(1.9) and obtain the occupation of the ground state

$$N_0 = N - 1 = \frac{T}{T_c} \frac{2}{6} \frac{1 + \ln N}{N} \quad (1.11)$$

Note that at  $T_c$  the particle density is  $(Nm)^{-1} = T_c$  and the de Broglie wavelength of particles  $\lambda_{dB} = \hbar/mT_c$  becomes comparable with the mean interparticle separation  $(Nm)^{-1/2} = T_c^{-1/2}$ . The result of Eq.(1.11) is similar to that in the 3D case and it was first obtained by Bagnato and Kleppner [7].

Above  $T_c$  one can omit the first term on the rhs of Eq.(1.9). The width of the cross-over region, i.e. the temperature interval where both terms on the rhs of Eq.(1.9) are equally important, is given by

$$\frac{T}{T_c} = \frac{\ln N}{N} \quad (1.12)$$

The Bose-condensed fraction of particles,  $N_0(T)/N$ , following from Eq.(1.9), is presented in Fig.1 for various values of  $N$ . For a large  $N$  the cross-over region is very narrow and one can speak of an ordinary BEC transition in an ideal harmonically trapped 2D gas.

For the 1D Bose gas in a harmonic potential  $V(z) = m\omega^2 z^2/2$ , the particle energy is  $E = \hbar\omega(j + 1/2)$ , with  $j$  being a non-negative integer, and the density of states is  $\rho(E) = 1/\hbar\omega$ . Here the integral representation of Eq.(1.7) fails as the integral diverges for  $\hbar\omega \rightarrow 0$ . Therefore, we should correctly take into account the discrete structure of the lowest energy levels. In the limit  $\hbar\omega \rightarrow 0$  we rewrite Eq.(1.1) in the form

$$N = N_0 + \frac{T}{\hbar\omega} \sum_{j=1}^{\infty} \frac{1}{j} + \sum_{j=M+1}^{\infty} \frac{1}{\exp(\hbar\omega(j + 1/2)/T) - 1} \quad (1.13)$$

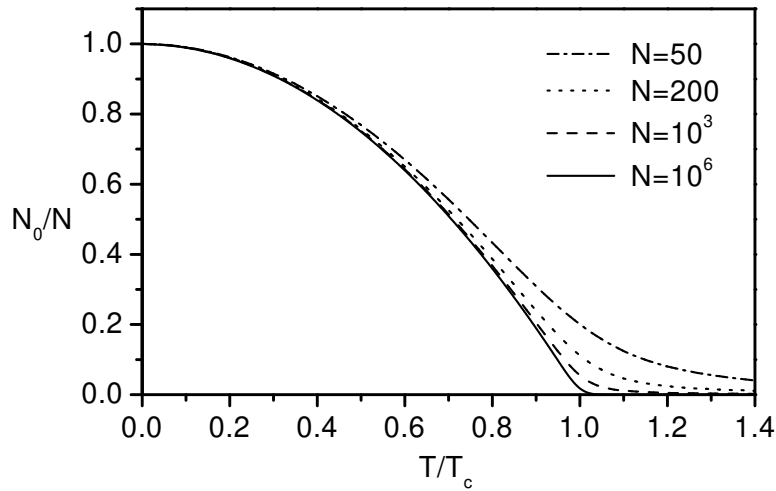


Fig. 1. The ground state population in a 2D trap versus temperature, calculated from Eq. (1.9).

where the number  $M$  satisfies the inequalities  $1 \leq M \leq T/\hbar\omega$ . The first sum is

$$\sum_{j=1}^M \frac{1}{j} = (M+1) \psi(M+1) - \psi(1) = (M+1) \psi(M+1) + \ln(M+1); \quad (1.14)$$

where  $\psi$  is the digamma function. The second sum in Eq.(1.13) can be transformed to an integral

$$\sum_{j=M+1}^{\infty} \frac{1}{\exp(j/T) - 1} = \frac{T}{\hbar\omega} \int_{M/T}^{\infty} \frac{dx}{\exp(x) - 1} = \frac{T}{\hbar\omega} \ln \frac{\Gamma(M+1)}{T}; \quad (1.15)$$

Finally, since in the limit of  $j \gg T$  the chemical potential is related to the population of the ground state as  $\mu = \hbar\omega \ln N_0$ , we reduce Eq.(1.13) to the form

$$N = \frac{T}{\hbar\omega} \ln \frac{T}{\hbar\omega} = N_0 \left( \frac{T}{\hbar\omega} + 1 + \frac{T}{\hbar\omega N_0} \right); \quad (1.16)$$

As in the 2D case, we have two regimes, with the border between them at a temperature

$$T_{1D} = \frac{N}{\ln N} \hbar\omega; \quad (1.17)$$

For temperatures below  $T_{1D}$ , the first term on the rhs of Eq.(1.15) greatly exceeds the second one and the ground state population behaves as

$$N_0 = N \frac{T}{\hbar\omega} \ln \frac{T}{\hbar\omega}; \quad (1.18)$$

The cross-over region is determined as the temperature interval where both terms are equally important:

$$\frac{T}{T_{1D}} = \frac{1}{\ln N}; \quad (1.19)$$

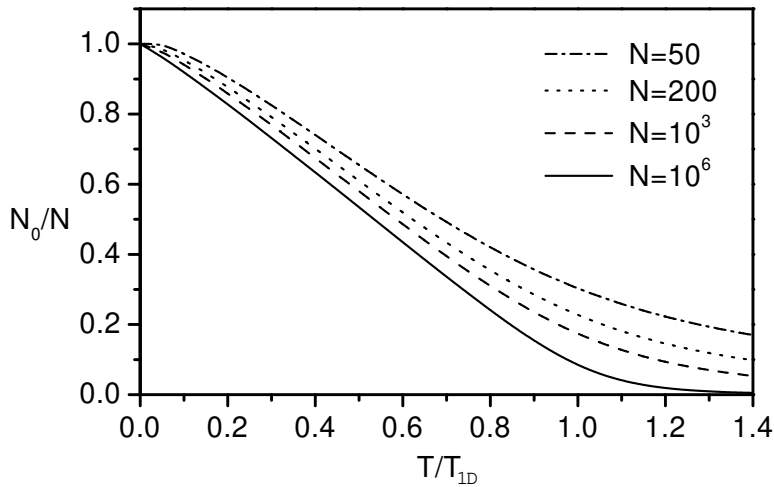


Fig. 2. The ground state population in a 1D trap versus temperature, found from Eq. (1.15).

In contrast to the 3D and 2D cases, the cross-over temperature is much lower than the degeneracy temperature  $T_d \sim N^{-1/2}$ . The described results have been obtained by Ketterle and van Duten [8]. In Fig 2 we present the relative occupation of the ground state  $N_0(T)/N$  calculated from Eq.(1.15).

The cross-over region in the 1D case is much wider than in 2D. This is not surprising as the cross-over is present only due to the discrete structure of the trap levels. The quasiclassical calculation does not lead to any sharp cross-over [7].

**Problem :** Describe the cross-over to the BEC regime in an ideal 2D gas of  $N$  identical bosons in a rectangular box with dimensions  $L_x; L_y$ . Find the cross-over temperature and the width of the cross-over region (E.B. Sonin, 1969).

## 2 LECTURE 2. INTERACTIONS AND BEC REGIMES IN 2D TRAPPED GASES

Interaction between particles drastically changes the picture of Bose-Einstein condensation in 2D and 1D gases. In the uniform 2D gas a true condensate can exist only at  $T = 0$  and, as mentioned in the Introduction, its absence at finite temperatures originates from long-wave fluctuations of the phase [1]. However, as was pointed out by Kane and Kadano [9] and then proved by Berezinskii [10], there is a superfluid phase transition at sufficiently low  $T$ . Kosterlitz and Thouless [11] found that this transition is associated with the formation of bound pairs of vortices below the critical temperature

$$T_{KT} = \frac{\hbar^2}{2m} n_s ; \quad (2.1)$$

where  $n_s$  is the superfluid density just below  $T_{KT}$ . This temperature is of the order of or smaller than  $T_d/4$ , where  $T_d = 2\hbar^2 n/m$  is the temperature of quantum degeneracy introduced in Lecture 1, and the notation  $n$  is used in this Lecture for the 2D density. Recent Monte Carlo calculations [12] established an exact relation between  $T_{KT}$  and  $T_d$  for the weakly interacting 2D Bose gas.

Early theoretical studies of 2D systems have been reviewed by Popov [1] and have led to the conclusion that below the Kosterlitz-Thouless transition temperature the Bose liquid (gas)

is characterized by the presence of a quasicondensate, that is a condensate with fluctuating phase (see, e.g., [13]). In this case the system can be divided into blocks with a characteristic size greatly exceeding the healing length but smaller than the phase coherence length. In each block one has a true condensate but the phases of different blocks are not correlated with each other.

The Kosterlitz-Thouless transition has been observed in monolayers of liquid helium [14], and recently the observation of this transition has been reported for the 2D gas of spin-polarized atomic hydrogen on liquid helium surface [15]. The Kosterlitz-Thouless transition is discussed in the lectures of Benoit Douçot.

In this Lecture we focus our attention on the interaction between particles and on the correlation properties of 2D Bose-condensed gases. Recently, the 2D regime was realized for trapped atomic Bose-Einstein condensates at MIT [16], LENS [17], Innsbruck [18], and JILA [19]. This was done by a tight optical confinement of the particle motion in one direction [16,17], or by a fast rotation of the cloud leading to an increase in the size of the sample in two directions [19]. We will focus special attention on how the nature of the Bose-condensed state is influenced by a finite size of the system.

## 2.1 Weakly interacting regime

We will consider weakly interacting gases with a short-range potential of interaction between particles. In this case the total interaction energy is equal to the sum of pair interactions and can be written as  $E_{\text{int}} = N^2 g/2$ , where  $g$  is the coupling constant for the pair interparticle interaction,  $N$  is the number of particles, and  $V$  the volume. Accordingly, the interaction energy per particle is equal to  $I = ng/2$ , with  $n$  being the 2D density.

Let us now discuss the conditions which are required for the 2D gas to be in the weakly interacting regime. The commonly used criterion assumes that the mean interparticle separation  $r$  greatly exceeds the characteristic radius of interaction between particles,  $R_e$ . In the 2D case we have  $r \sim (2/n)^{1/2}$  and thus obtain the inequality

$$n R_e^2 \ll 1 : \quad (2.2)$$

The weakly interacting regime requires that at interparticle distances of the order of  $r$ , the wavefunction of particles is not influenced by the interaction between them. Relying on this requirement, we develop a physical picture which will be used for finding how the criterion of the weakly interacting regime depends on the dimensionality of the system. We consider a box of size  $r$ , which on average contains one particle. In the limit of  $T \rightarrow 0$ , the particle kinetic energy is  $K \sim \hbar^2 / m r^2$ . The wavefunction of the particle is not influenced by the interparticle interaction if  $K$  is much larger than the interaction energy per particle,  $I = ng/2$ . The inequality  $K \gg I$  immediately gives the criterion of the weakly interacting regime in terms of the density and coupling constant. In the 2D case this criterion takes the form

$$\frac{m \hbar^2}{2} \frac{1}{n^2} \gg 1 : \quad (2.3)$$

In the 2D gas at  $T \rightarrow 0$  the coupling constant is (see, e.g., [1])

$$g = \frac{4 \hbar^2}{m} \frac{1}{\ln(1/n d^2)} ; \quad (2.4)$$

where a length  $d$  depends on the shape of the interatomic potential and in the absence of scattering resonances is of the order of  $R_e$ . Then, from Eq.(2.3) we immediately arrive at the

criterion (2.2). However, on approach to a resonance, the value of  $d$  is quite different from  $R_e$ , and one should return to the criterion (2.3).

In the dilute limit Eq.(2.4) gives  $g > 0$ , except for the case where a weakly bound state of colliding atoms is present. Then the length  $d$  is extremely large and even at very low densities one can have the condition  $nd^2 \sim 1$  leading to an attractive mean-field interaction ( $g < 0$ ). However, in this case the 2D Bose gas at  $T \rightarrow 0$  is unstable with regard to collapse.

Note that in the 3D case we have the coupling constant  $g_{3D} = 4\pi\hbar^2 a/m$  and  $r_{3D} = n_{3D}^{-1/3}$ , with  $n_{3D}$  being the 3D density, and  $a$  the 3D scattering length. The condition  $K \ll |J|$  then leads to the well-known criterion  $na^3 \ll 1$ , required for the weakly interacting regime in the 3D gas. In the absence of resonances, the 3D scattering length is of the order of  $R_e$  and this criterion is equivalent to the inequality  $R_e \ll r$ .

In ongoing experiments, two-dimensional atomic gases are obtained by (tightly) confining the motion of particles in one direction to zero point oscillations [16,18] and, in this respect, can be called quasi2D [20]. Kinetically the gas is two-dimensional, but the value of an effective 2D coupling constant  $g$  for the interparticle interaction depends on the particle motion in the tightly confined direction.

Let us first make a qualitative analysis of the interactions in such quasi2D gas. It can be viewed as a 3D gas which is uniform in two directions ( $x$  and  $y$ ), and is confined to zero point oscillations by a harmonic potential  $m \frac{1}{2} \omega_z^2 z^2$  in the third direction ( $z$ ). The quasi2D regime requires the inequality

$$\hbar \omega_z \ll n_{2D} |J|; \quad (2.5)$$

where  $n$  is the number of particles per unit area in the  $x-y$  plane and represents the 2D density of the quasi2D gas. Then the distribution of the density in the  $z$  direction is not influenced by the interactions and is given by

$$n_{3D}(z) = \frac{n}{\sqrt{l_0}} \exp\left(-\frac{z^2}{l_0^2}\right); \quad (2.6)$$

with  $l_0 = (\hbar/m \omega_z)^{1/2}$  being the harmonic oscillator length. The average interaction energy per particle is obtained by averaging the 3D interaction over the density profile in the  $z$  direction:

$$I = \frac{g_{3D} \int_{-\infty}^{\infty} n_{3D}^2(z) dz}{\int_{-\infty}^{\infty} n_{3D}(z) dz} = ng; \quad (2.7)$$

Eqs. (2.6) and (2.7) lead to the following relation for the effective coupling constant:

$$g = \frac{2\pi\hbar^2 a}{m l_0}; \quad (2.8)$$

Accordingly, the criterion of the weakly interacting regime given by Eq.(2.3) takes the form

$$l_0 \ll |J|; \quad (2.9)$$

One can easily check that under conditions (2.5) and (2.9) the gas satisfies the 3D criterion of weak interactions,  $n_{3D} a^3 \ll 1$ .

The criterion (2.9) is independent of the gas density and in this respect is different from the criterion of the weakly interacting regime in the purely 2D case, following from Eqs. (2.3) and (2.4). The density enters the problem only through the condition of the quasi2D regime given by Eq.(2.5). However, the above analysis does not take into account the 2D character of the particle motion at large distances between them. In the next section we discuss the quasi2D scattering problem and derive a more exact criterion of weak interactions in the quasi2D case.



## 2.2 Quasi2D scattering problem

Collisional properties of cold atoms strongly confined in one direction have been of great interest in the studies of spin-polarized atomic hydrogen. The interest was related to inelastic and elastic collisions in the 2D gas of hydrogen atoms adsorbed on liquid helium surface (see [21] for review). The creation of atomic gases in the quasi2D regime [16{19] opens new handles on studying 2D features of interparticle collisions, and provides spectacular evidence for the relation between the quasi2D scattering parameters and those in 3D. Theoretical studies of elastic and inelastic interactions in the quasi2D regime have been performed in [20,22,23], and it has been shown how a decrease of the tight confinement transforms this regime into the 3D one [22].

Here we consider elastic scattering of two atoms in the quasi2D regime [22]. So, the atoms are (tightly) confined to zero point oscillations in the axial ( $z$ ) direction, and their motion in two other ( $x, y$ ) directions is free at a large separation in the  $x-y$  plane. For a harmonic axial confinement, the motion of two atoms interacting with each other via the potential  $U(r)$  can be still separated into their relative and center-of-mass motion. The latter drops out of the scattering problem. The relative motion is governed by the potential  $U(r)$  and by the potential  $V_H(z) = m \frac{1}{2} \omega_0^2 z^2$  originating from the axial confinement with frequency  $\omega_0$ . In the quasi2D regime one has the condition

$$\hbar \omega_0 \gg \epsilon; \quad (2.10)$$

where  $\epsilon = \hbar^2 q^2 / m$  and  $q$  are the energy and wavevector of the motion in the  $x-y$  plane. Therefore, the atoms are in the ground state of the potential  $V_H(z)$  both in the incident and the scattered wave. The wavefunction of the relative motion satisfies the Schrodinger equation

$$\frac{\hbar^2 \nabla^2}{m} \psi + U(r) + V_H(z) \psi = \frac{\hbar^2 q^2}{2} \psi(r) = \epsilon \psi(r); \quad (2.11)$$

We will consider the ultracold limit where the characteristic de Broglie wavelength of atoms greatly exceeds the radius of interatomic interaction  $R_e$ . For the motion in the  $x-y$  plane the de Broglie wavelength is  $\lambda = \hbar/q$ , and we immediately obtain the inequality  $q R_e \ll 1$ . Under this condition the scattering is determined by the contribution of the  $s$ -wave for the motion in the  $x-y$  plane. In the axial direction, the atoms are tightly confined and the axial harmonic oscillator length  $l_0$  plays the role of their axial de Broglie wavelength. Therefore, we also require the condition

$$l_0 \gg R_e; \quad (2.12)$$

which will allow us to consider only the  $s$ -wave for the three-dimensional relative motion of the atoms when they approach each other to short distances. The condition of the quasi2D regime (2.10) can be also written as  $q l_0 \ll 1$ , and one clearly sees that Eqs. (2.10) and (2.12) automatically lead to the inequality  $q R_e \ll 1$ .

The scattering amplitude is determined through the asymptotic form of the wavefunction at an infinite separation in the  $x-y$  plane, where it is represented as a superposition of an incident and scattered wave:

$$\psi(r) = \psi'_0(z) e^{iqz} + f(q; \theta) \frac{i}{8q} e^{iqz}; \quad (2.13)$$

where  $\psi'_0(z) = (1/2\pi l_0^2)^{1/4} \exp(-z^2/4l_0^2)$  is the eigenfunction of the ground state in the potential  $V_H(z)$ , and  $\theta$  is the scattering angle. The  $s$ -wave scattering is circularly symmetric in the  $x-y$

plane, and the scattering amplitude is independent of  $\theta$ . Note that  $f(q; \theta)$  in Eq.(2.13) is different by a factor of  $\sqrt{\frac{p}{8q}}$  from the definition of the 2D scattering amplitude used in [24].

Relying on the condition (2.12) we will express the scattering amplitude through the 3D scattering length. At interparticle distances  $r \gg R_e$  the relative motion in the  $x-y$  plane is free, and the motion along the  $z$  axis is governed only by the harmonic potential  $V_H(z)$ . Then, the solution of Eq.(2.11) with  $U(r) = 0$  can be expressed through the Green function  $G^+(r; r^0)$  of this equation. Retaining only the  $s$ -wave for the motion in the  $x-y$  plane, we have

$$\psi(r) = \sqrt{\frac{p}{8q}} J_0(qr) - f G^+(r; 0) = \psi_0(0) : \quad (2.14)$$

For  $\theta \rightarrow 1$  the Green function is  $G^+(r; 0) = \psi_0(z) \psi_0(0) \sqrt{\frac{p}{8q}} \exp(iqz)$  and Eq.(2.14) gives the  $s$ -wave of Eq.(2.13).

The condition  $l_0 \gg R_e$  ensures that the relative motion of atoms in the region of interatomic interaction is not influenced by the axial (tight) confinement. Therefore, the wavefunction  $\psi(r)$  at distances  $R_e \ll r \ll l_0$  differs only by a normalization coefficient from the 3D wavefunction of free motion at zero energy,  $\psi_{3D}(r)$ . Writing this coefficient as  $\sqrt{\frac{p}{8q}} \psi_0(0)$  and recalling that for  $r \gg R_e$  one has  $\psi_{3D}(r) = (1 - a/r)$ , we obtain

$$\psi(r) = \sqrt{\frac{p}{8q}} \psi_0(0) \left(1 - \frac{a}{r}\right) ; \quad R_e \ll r \ll l_0 : \quad (2.15)$$

Eq.(2.15) contains the 3D scattering length  $a$  and serves as a boundary condition for  $\psi(r)$  (2.14) at  $r \rightarrow 0$ .

For  $r \rightarrow 0$ , a straightforward calculation of the Green function  $G^+(r; 0)$  yields [20,22]

$$G^+(r; 0) = \frac{1}{4r} + \frac{1}{2(2 - \sqrt{2})^3 l_0} \ln \frac{B \sim \sqrt{2}}{r} + i ; \quad (2.16)$$

where  $B \sim 0.915$ . With the Green function (2.16), the wavefunction (2.14) at  $r \rightarrow 0$  should coincide with  $\psi(r)$  (2.15). This gives the coefficient and the scattering amplitude:

$$f(\sqrt{2}) = 4 \sqrt{\frac{p}{8q}} \psi_0^2(0) a = \frac{2 \sqrt{\frac{p}{8q}}}{l_0 = a + (1 - \sqrt{2}) [\ln(B \sim \sqrt{2}) + i]} : \quad (2.17)$$

One can see from Eq.(2.17) that the scattering amplitude is a universal function of the parameters  $a=l_0$  and  $\sqrt{2} \sim \sqrt{2}$ .

The 2D kinematics of the relative motion at interatomic distances  $r > l_0$  manifests itself in the appearance of logarithmic dependence of the scattering amplitude on  $\sqrt{2} \sim \sqrt{2}$ . The quasi2D scattering amplitude can be represented in the purely 2D form obtained, for example, in [24]:

$$f(q) = \frac{2}{\ln(1 - qd) + i\sqrt{2}} : \quad (2.18)$$

In the purely 2D case a characteristic length  $d$  depends on the shape of the interatomic potential  $U(r)$ . For the considered quasi2D regime this length is expressed through  $l_0$  and the 3D scattering length  $a$ :

$$d = \frac{d}{2} e^C = \frac{r}{B} l_0 \exp \left( - \frac{r}{2a} l_0 \right) ; \quad (2.19)$$

where  $C$  is the Euler's constant.

We thus conclude that the scattering problem in the quasi2D regime is equivalent to the scattering in an effective purely 2D potential which leads to the same value of  $d$ . For a negative

a satisfying the condition  $|a| \ll l_0$ , the effective potential is a shallow well which has a depth  $|V_0|$  and a radius  $l_0$ . This shallow well supports a weakly bound state with an exponentially small binding energy  $\epsilon_0$ , which leads to an exponentially large  $d$  as follows from Eq.(2.19). As a result, we have a resonance energy dependence of the scattering amplitude  $f$  at a fixed ratio  $a=l_0$ , and a resonance behavior of  $f$  as a function of  $a=l_0$  at a fixed  $\epsilon_0 \approx \epsilon_0$ .

Equation (2.17) shows that the resonance is achieved at  $a = a(\epsilon_0) = \frac{1}{2} l_0 = \ln(B \epsilon_0)$ . One can think of observing the resonance dependence of  $f$  on  $a=l_0$  by measuring the rate of elastic collisions, which is proportional to  $|f|^2$ . For example, one can keep temperature and  $\epsilon_0$  constant and vary  $a$  by using Feshbach resonances. This will be a striking difference from the 3D case, where the rate constant of elastic collisions monotonically increases with  $a^2$ .

Stanford [25,26] and ENS [27,28] experiments with a thermal gas of Cs atoms tightly confined in one direction, observed a pronounced deviation of collisional rates from the 3D behavior. In these experiments the temperature was of the order of  $\epsilon_0$  and, in this respect, they were in between the quasi2D and 3D regimes.

The scattering amplitude  $f$  determines the coupling constant  $g$  for a fixed collision energy  $\epsilon$ . Away from the resonance, one may omit the imaginary part in Eq.(2.17) and  $f$  becomes real. Using Eq.(2.11) one can establish that in the ultracold limit the interaction energy for a pair of atoms is equal to  $g = \epsilon$ , where the coupling constant is given by

$$g = \int d^3r' \int_0^\infty dz U(r) \psi(r, z); \quad (2.20)$$

and  $\psi$  is the volume of the system. Accordingly, the total interaction energy is equal to  $g = \epsilon$  multiplied by the number of pairs  $N^2/2$ , as stated in the beginning of this Lecture.

The main contribution to the integral in Eq.(2.20) comes from interparticle distances  $r \ll R_e$ . Therefore, one may put  $\psi_0(z) = \psi_0(0)$  and  $\psi(r) = \psi_0(0) \psi_{3D}(r)$ . Then, using the well-known result  $\int d^3r \psi_{3D}(r) U(r) = 4\pi a/m$  and Eq.(2.17), we obtain

$$g = \frac{\epsilon^2 f(\epsilon)}{m} = \frac{4\pi \epsilon^2}{m} \frac{1}{2 l_0 = a + \ln(B \epsilon_0)}; \quad (2.21)$$

As one can see, the coupling constant for the interaction between particles depends on their relative energy. In a thermal gas, averaging the coupling constant over the energy distribution of particles simply leads to the replacement of  $\epsilon$  by  $T$  in Eq.(2.21).

In a Bose-condensed 2D gas, similarly to the 3D case (see, e.g. [29]), to zero order in perturbation theory the coupling constant is equal to the vertex of interparticle interaction in vacuum at zero momenta and frequency  $\epsilon = 2\epsilon_0$ . For low  $\epsilon_0 > 0$  this vertex coincides with the amplitude of scattering at relative energy  $\epsilon$  and, hence, is given by Eq.(2.5) with  $\epsilon = 2\epsilon_0$ . This certainly requires the quasi2D condition  $\epsilon_0 \ll \epsilon$ . For  $\epsilon_0 < 0$ , analytical continuation of Eq.(2.21) to  $\epsilon_0 < 0$  leads to the replacement  $\epsilon_0 \rightarrow |\epsilon_0|$ .

We can now analyze the criterion of the weakly interacting regime for the ultracold quasi2D gas, assuming that it is dilute and the condition  $n R_e^2 \ll 1$  is fulfilled. Since the scattering amplitude  $f$  and, hence, the coupling constant  $g$  can be written in the purely 2D form (see Eq.(2.18)), the weakly interacting regime requires the inequality  $m |g| \ll \epsilon^2$  given above by Eq.(2.3). For  $a > 0$ , the quasi2D resonance is absent and this inequality is satisfied for any ratio  $a=l_0$ . For a negative  $a$ , the system should be far away from the resonance and one should use Eq.(2.21) to make sure that the condition (2.3) is satisfied. This is demonstrated in Fig.3 where we present the parameter  $m |g| \epsilon^2$  as a function of the ratio  $a=l_0$ . The results are obtained from Eq.(2.21) for a fixed ratio  $\epsilon_0/\epsilon = 10^3$ . In the vicinity of the resonance, where the criterion  $m |g| \epsilon^2 \ll 1$  is not satisfied, they are shown by the dashed curves.

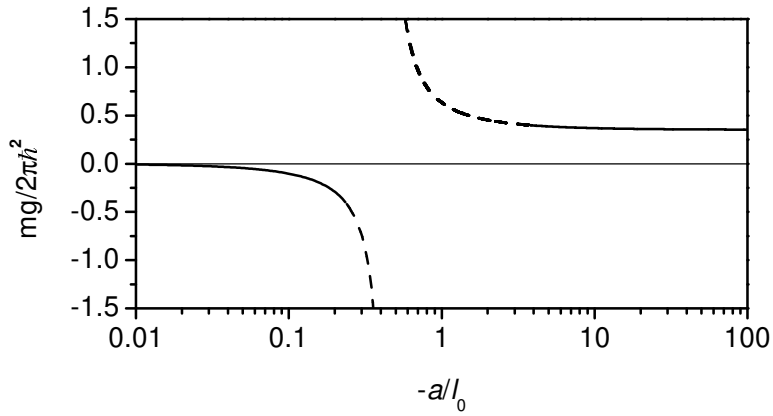


Fig. 3. The parameter  $mg/2\pi\hbar^2$  versus  $-a/l_0$ , obtained from Eq.(2.21) (see text).

### 2.3 True BEC at $T = 0$

We start the discussion of BEC regimes in (quasi)2D weakly interacting gases with the case of zero temperature. From this point on we consider only repulsive interaction between particles ( $g > 0$ ). The behavior of attractively interacting Bose gases and, in particular, the problem of collapses are beyond the scope of these lectures.

In the second quantization the Hamiltonian of the system reads:

$$\hat{H} = \int d\mathbf{r} \hat{\psi}^\dagger \left( \frac{\hbar^2 \nabla^2}{2m} + V(\mathbf{r}) + \frac{g}{2} \hat{\psi}^\dagger \hat{\psi} \right) \hat{\psi}; \quad (2.22)$$

where  $\hat{\psi}(\mathbf{r};t)$  is the Heisenberg field operator of the atoms,  $V(\mathbf{r})$  is an external (trapping) potential, and all field operators in the integrand are taken at the same position  $\mathbf{r}$  and for the same time  $t$ . The Heisenberg equation of motion for the field operator takes the form:

$$i\hbar \frac{\partial \hat{\psi}}{\partial t} = [\hat{\psi}; \hat{H}] = \frac{\hbar^2 \nabla^2}{2m} \hat{\psi} + V(\mathbf{r}) \hat{\psi} + g \hat{\psi}^\dagger \hat{\psi} \hat{\psi}; \quad (2.23)$$

We now assume a priori that there is a true condensate at  $T = 0$ , and the condensate density  $n_0$  is much larger than the density of non-condensed particles  $n^0$ . Accordingly, we represent the field operator as a sum of the non-condensed part  $\hat{\psi}^0$  and the condensate wavefunction  $\psi_0 = \sqrt{n_0} \hat{\psi}_0$  which is a c-number:

$$\hat{\psi} = \hat{\psi}^0 + \psi_0; \quad (2.24)$$

At equilibrium, the time dependence of the condensate wavefunction is reduced to  $\psi_0 / \exp(-i\epsilon t/\hbar)$ , where  $\epsilon$  is the chemical potential. Then, taking average of both sides of Eq.(2.23) and omitting the contribution of non-condensed particles, we obtain the Gross-Pitaevskii equation for the condensate wavefunction [30,31]:

$$\frac{\hbar^2 \nabla^2}{2m} \psi_0 + V(\mathbf{r}) \psi_0 + g n_0 \psi_0 = \epsilon \psi_0; \quad (2.25)$$

The function  $\psi_0$  is normalized by the condition

$$\int d\mathbf{r} |\psi_0|^2 = N; \quad (2.26)$$

which gives a relation between the number of particles  $N$  and chemical potential  $\mu$ .

Equations (2.23) and (2.25) immediately lead to the equation of motion for the non-condensed part of the field operator:

$$i\hbar \frac{\partial \psi}{\partial t} = \frac{\hbar^2 \nabla^2}{2m} \psi + V(\mathbf{r}) \psi + 2g \psi_0 \psi^2 + g \psi_0^2 \psi^4 : \quad (2.27)$$

We then use the Bogoliubov transformation (see [32]) generalized for the spatially non-uniform case [33] and express  $\psi$  through the eigenmodes of elementary excitations:

$$\psi = \exp(i\mu t/\hbar) \sum_{\mathbf{k}} u_{\mathbf{k}} \hat{a}_{\mathbf{k}} \exp(-i\epsilon_{\mathbf{k}} t/\hbar) + v_{\mathbf{k}} \hat{a}_{\mathbf{k}}^\dagger \exp(i\epsilon_{\mathbf{k}} t/\hbar) : \quad (2.28)$$

Here  $\hat{a}_{\mathbf{k}}; \hat{a}_{\mathbf{k}}^\dagger$  are annihilation and creation operators of the excitations, and  $\epsilon_{\mathbf{k}}$  are their eigenenergies. Excitations are characterized by a set of quantum numbers  $\mathbf{k}$ , and their Bogoliubov functions  $u_{\mathbf{k}}; v_{\mathbf{k}}$  are normalized by the condition

$$\int d\mathbf{r} |u_{\mathbf{k}}(\mathbf{r})|^2 - |v_{\mathbf{k}}(\mathbf{r})|^2 = 1 : \quad (2.29)$$

Combining both sides of Eq. (2.27) with the operators  $\hat{a}_{\mathbf{k}}$  and  $\hat{a}_{\mathbf{k}}^\dagger$ , we arrive at the Bogoliubov-de Gennes equations for the excitation energies and wavefunctions. Assuming that aside from the factor  $\exp(-i\mu t/\hbar)$ , the condensate wavefunction  $\psi_0$  is real, these equations read:

$$\frac{\hbar^2 \nabla^2}{2m} u + V(\mathbf{r}) u + g \psi_0^2 u = \epsilon_{\mathbf{k}} u \quad f^+ = \epsilon_{\mathbf{k}} f \quad (2.30)$$

$$\frac{\hbar^2 \nabla^2}{2m} v + V(\mathbf{r}) v + 3g \psi_0^2 v = \epsilon_{\mathbf{k}} v \quad f = \epsilon_{\mathbf{k}} f^+ ; \quad (2.31)$$

where the functions  $f = u - v$ .

In the spatially uniform case Eq. (2.25) is reduced to the expression for the chemical potential through the condensate density:  $\mu = n_0 g$ . Excitations are characterized by their wave vector  $\mathbf{k}$ , and Eqs. (2.30), (2.31) give the eigenfunctions

$$f_{\mathbf{k}} = u_{\mathbf{k}} \quad v_{\mathbf{k}} = \frac{1}{E_{\mathbf{k}}} \frac{\epsilon_{\mathbf{k}}}{E_{\mathbf{k}}} \exp(i\mathbf{k} \cdot \mathbf{r}) \quad (2.32)$$

and lead to the Bogoliubov energy spectrum

$$\epsilon_{\mathbf{k}} = \sqrt{E_{\mathbf{k}}^2 + 2 E_{\mathbf{k}} \mu} ; \quad (2.33)$$

where  $E_{\mathbf{k}} = \hbar^2 k^2 / 2m$  is the energy of a free particle. For small momenta, excitations are phonons characterized by a linear dispersion law  $\epsilon_{\mathbf{k}} = \hbar c_s k$ , where  $c_s = \sqrt{\mu/m}$  is the velocity of sound. High-momentum excitations are single particles with  $\epsilon_{\mathbf{k}} = E_{\mathbf{k}} + \mu$ . Characteristic momenta at which the linear spectrum transforms into the quadratic one are of the order of  $1/l_c$ , where  $l_c = \hbar / \sqrt{2m\mu}$  is called correlation or healing length. The corresponding excitation energies are  $\mu$ . Note that the criterion (2.3) of the weakly interacting regime is equivalent to the condition  $l_c \gg r$ . In other words, there are many particles under the healing length.

We now calculate the density of non-condensed particles  $n^0$  and the single-particle correlation function. Using Eqs. (2.28) and (2.32) we obtain

$$n^0 = \langle \psi^\dagger(\mathbf{r}) \psi(\mathbf{r}) \rangle = \sum_{\mathbf{k}} \frac{d^3 k}{(2\pi)^3} v_{\mathbf{k}}^2 = \frac{m g}{4 \hbar^2} n_0 : \quad (2.34)$$

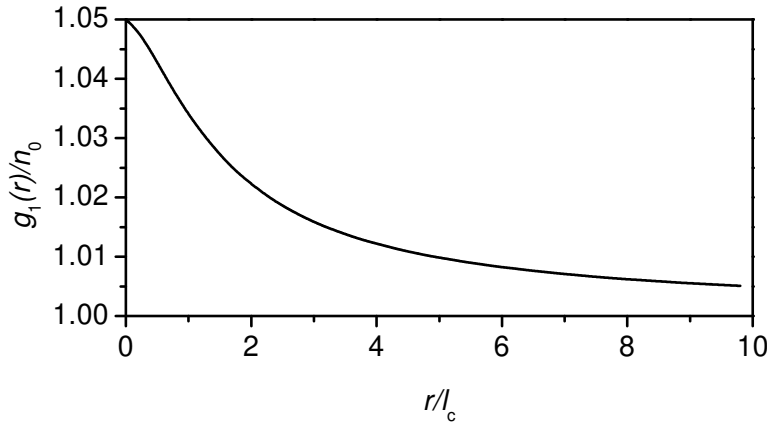


Fig. 4. Normalized single-particle correlation function  $g_1(r)/n_0$  versus  $r/l_c$ , for a uniform 2D Bose gas at zero temperature.

One clearly sees that the ratio  $n^0/n_0$  is small. It is proportional to the small parameter  $g=2/\lambda^2$  required for the weakly interacting regime in the 2D Bose gas.

The single-particle correlation function is  $g_1(r^0; r^0) = \langle \hat{\psi}^\dagger(r^0) \hat{\psi}(r^0) \rangle$  and it depends only on the relative coordinate  $r = r^0 - r^0$ . On the basis of Eqs. (2.24), (2.28), and (2.32) we obtain

$$g_1(r) = n_0 + \frac{1}{(2\pi)^2} \int d^2k v_k^2 \exp(ik \cdot r) = n_0 \left[ 1 + \frac{mg}{2\lambda^2} I_1\left(\frac{r}{l_c}\right) - K_1\left(\frac{r}{l_c}\right) \right]; \quad (2.35)$$

where  $I_1$  and  $K_1$  are the growing and decaying modified Bessel functions, respectively. The result of Eq.(2.35) is displayed in Fig.4. For  $r \ll l_c$  the single-particle correlation function is close to the total density  $n$ . At distances  $r \gg l_c$ , Eq.(2.35) gives

$$g_1(r) = n_0 \left[ 1 + \frac{mg}{4\lambda^2} \frac{l_c}{r} \right]; \quad r \gg l_c; \quad (2.36)$$

For  $r \gg l_c$  the second term in the brackets vanishes and  $g_1$  is tending to  $n_0$ . Thus, there is a long-range order in the system. This justifies our initial assumption of the presence of a true BEC in the 2D weakly interacting gas at  $T = 0$ . Note that  $g_1$  drops from  $n$  to  $n_0$  at distances of the order of the healing length  $l_c$ .

In order to go beyond the Bogoliubov approach and find, for example, corrections to the excitation energies, which are small as  $g=2/\lambda^2$ , one may proceed along the lines of the Beliaev theory [34] developed for 3D Bose-condensed gases at  $T = 0$ .

#### 2.4 Quasiconsensate at finite temperatures

As we already mentioned, the finite-temperature uniform 2D Bose gas is characterized by the absence of a true Bose-Einstein condensate and long-range order. To gain insight into the nature of this phenomenon we first try to calculate the density of non-condensed particles, assuming that there is a true BEC and one can use the Bogoliubov approach described in the previous subsection. Then, at finite temperatures, from Eqs. (2.28) and (2.32) we obtain

$$n^0 = \langle \hat{\psi}^\dagger(r) \hat{\psi}(r) \rangle = n_v^0 + n_T^0; \quad (2.37)$$

The vacuum (temperature-independent) contribution  $n_v^0$  is given by Eq.(2.34), and the thermal contribution is determined by the relation

$$n_T^0 = \frac{Z}{(2\pi)^2} (v_k^2 + u_k^2) N_k = \frac{Z}{(2\pi)^2} \frac{E_k + \epsilon_k}{\epsilon_k} N_k ; \quad (2.38)$$

where  $N_k = [\exp(\epsilon_k/T) + 1]^{-1}$  are equilibrium occupation numbers for the excitations. For  $k \neq 0$  the occupation numbers are  $N_k = T/\epsilon_k$ , and the excitation energy is  $\epsilon_k = \hbar \omega_k$ . Therefore, the integrand in the rhs of Eq.(2.38) behaves as  $d^2k/k^2$  and the integral is divergent at small momenta, which rules out the assumption of the presence of a true condensate. The origin of this infrared divergence is related to long-wave fluctuations of the phase of the condensate wavefunction, which can be understood turning to the density-phase representation for the field operators:

$$\hat{\psi} = \exp(i\hat{\phi}) \hat{\rho}^{1/2}; \quad \hat{\psi}^\dagger = \hat{\rho}^{1/2} \exp(-i\hat{\phi}) ; \quad (2.39)$$

Here the density and phase operators are real and satisfy the commutation relation

$$[\hat{\rho}(r); \hat{\phi}(r')] = i \delta(r - r') ; \quad (2.40)$$

We now present a general approach which is based on the Hamiltonian (2.22) and includes the presence of an external trapping potential  $V(r)$ . We assume a priori and justify later that fluctuations of the density are small. Substituting Eqs. (2.39) into Eq. (2.23) and separating real and imaginary parts, we get the coupled continuity and Euler hydrodynamic equations for the density and velocity  $\hat{v} = (\hbar/m)r \hat{\phi}$ :

$$\frac{\partial \hat{\rho}^{1/2}}{\partial t} = \frac{\hbar^2}{2m} (\hat{\phi}^{1/2} \hat{\rho}^{1/2} + 2r \hat{\phi}^{1/2} \hat{\rho}^{1/2}) ; \quad (2.41)$$

$$\frac{\partial \hat{\phi}^{1/2}}{\partial t} = \frac{\hbar^2}{2m} (r \hat{\phi}^{1/2})^2 \hat{\rho}^{1/2} - \frac{\hbar^2}{2m} \hat{\rho}^{1/2} + V(r) \hat{\rho}^{1/2} + g \hat{\rho}^{3/2} ; \quad (2.42)$$

For small density fluctuations, Eq.(2.41) shows that fluctuations of the phase gradient are also small. Writing the density operator as  $\hat{\rho}(r) = \bar{n}(r) + \delta \hat{\rho}(r)$  and shifting the phase by  $\phi \rightarrow \phi + \phi_0$ , we then linearize Eqs. (2.41-2.42) with respect to  $\delta \hat{\rho}, \delta \hat{\phi}$  around the stationary solution  $\bar{n} = n, \delta \hat{\phi} = 0$ . The zero order terms give the Gross-Pitaevskii equation for the mean density  $n$ :

$$\frac{\hbar^2}{2m} \nabla^2 \frac{\bar{n}}{\bar{n}} + V(r) + gn = \mu ; \quad (2.43)$$

and the first order terms provide equations for the density and phase fluctuations:

$$\frac{\partial \delta \hat{\rho}^{1/2}}{\partial t} = \left( \frac{\hbar^2}{2m} \nabla^2 + V(r) + gn \right) \delta \hat{\rho}^{1/2} ; \quad (2.44)$$

$$\frac{\partial \delta \hat{\phi}^{1/2}}{\partial t} = \left( \frac{\hbar^2}{2m} \nabla^2 + V(r) + 3gn \right) \delta \hat{\phi}^{1/2} ; \quad (2.45)$$

Solutions of Eqs. (2.44-2.45) for  $\delta \hat{\rho}, \delta \hat{\phi}$  are obtained in terms of elementary excitations:

$$\delta \hat{\rho}(r) = \sum_{\mathbf{k}} \bar{n}^{1/2} f_{\mathbf{k}}(r) e^{i\mathbf{k} \cdot \mathbf{r} - i\epsilon_{\mathbf{k}} t} \hat{a} + \text{h.c.} ; \quad (2.46)$$

$$\delta \hat{\phi}(r) = \sum_{\mathbf{k}} [4n(r)]^{1/2} f_{\mathbf{k}}^*(r) e^{i\mathbf{k} \cdot \mathbf{r} - i\epsilon_{\mathbf{k}} t} \hat{a} + \text{h.c.} ; \quad (2.47)$$

where the eigenfunctions  $f_{\mathbf{k}}$  obey the Bogoliubov-de Gennes equations (2.30) and (2.31), with  $j_0^2$  replaced by  $n$ . In the previous subsection these functions were introduced as eigenfunctions of elementary excitations of a true Bose-Einstein condensate. We thus see that the

assumption of small density fluctuations is sufficient for having the Bogoliubov wavefunctions and spectrum of the excitations, irrespective of the presence or absence of a true condensate. Note that this statement holds for both uniform and trapped Bose gases in the weakly interacting regime in any dimension.

In the uniform case the chemical potential is  $\mu = \epsilon_0$ , and the excitation wavefunctions and spectrum are given by Eqs. (2.32) and (2.33). As discussed above, the characteristic excitation energies at which the character of the spectrum transforms from the phonon into the single-particle one are of the order of  $\epsilon_0$ . We, therefore, separate the energy space into two regions: low-energy (phonon) part with  $\epsilon_k < \epsilon_0$ , and high-energy (free-particle) part where  $\epsilon_k > \epsilon_0$ . The operators of the density and phase fluctuations are then represented as:

$$\hat{n} = \hat{n}_p + \hat{n}_f; \quad (2.48)$$

$$\hat{\phi} = \hat{\phi}_p + \hat{\phi}_f; \quad (2.49)$$

where the indices p and f stand for the phonon ( $\epsilon_k < \epsilon_0$ ) and free-particle ( $\epsilon_k > \epsilon_0$ ) parts, respectively.

Fluctuations originating from the high-energy part are small. This is seen from the calculation of the density of this part of the gas,  $\langle \hat{n}_f^y \hat{n}_f \rangle$ , where the operator  $\hat{n}_f$  accounts for both the density and phase fluctuations and is given by the Bogoliubov transformation (2.28) in which the summation is performed only over excitations with energies  $\epsilon_k > \epsilon_0$ . At energies significantly larger than  $\epsilon_0$  the function  $v_k = (\epsilon_k^+ - \epsilon_k^-)/2 \approx \epsilon_0$ , and  $u_k = (\epsilon_k^+ + \epsilon_k^-)/2 \approx \epsilon_0 \exp(ik \cdot r)$ . The excitation energy is  $\epsilon_k \approx \epsilon_0 + \frac{\hbar^2 k^2}{2m}$  and, hence, the operator  $\hat{n}_f$  describes an ideal thermal gas of Bose particles with chemical potential equal to  $\epsilon_0$ . The density of this gas is exponentially small at  $T < T_d$ . In the 2D case, for higher temperatures it is equal to

$$\langle \hat{n}_f^y \hat{n}_f \rangle \approx \int_{\epsilon_k > \epsilon_0} \frac{d^2 k}{(2\pi)^2} N_k < n \frac{T}{T_d} \ln \frac{T}{T_d};$$

and is much smaller than  $n$  assuming that  $T$  is well below the temperature of quantum degeneracy  $T_d = 2\pi \hbar^2 / m k_B$ .

The low-energy fluctuations of the density at  $T \approx T_d$  are also small. This follows from the calculation of the density-density correlation function  $\langle \hat{n}_p(r) \hat{n}_p(0) \rangle$ . For the 2D gas, a straightforward calculation using Eq. (2.46) yields

$$\frac{\langle \hat{n}_p(r) \hat{n}_p(0) \rangle}{n^2} = \frac{1}{n} \sum_{\epsilon_k < \epsilon_0} \frac{E(k)}{\epsilon(k)} (2N_k + 1) \cos(k \cdot r) < \max \left\{ \frac{T}{T_d}; \frac{mg}{4\pi^2} \right\} \quad (2.50)$$

Similarly, one finds that the density-phase correlation functions  $\langle \hat{n}_p(r) \hat{\phi}_p(0) \rangle$  and  $\langle \hat{\phi}_p(r) \hat{n}_p(0) \rangle$  are small for  $T \approx T_d$ .

To zero order in perturbation theory, omitting small high-energy fluctuations and small low-energy fluctuations of the density, the single-particle correlation function is found by using the field operator in the form:

$$\hat{\psi} = \sqrt{n} \exp(i\hat{\phi}_p); \quad (2.51)$$

Relying on the Taylor expansion of the exponent one proves directly that  $\langle \hat{\psi}^\dagger(r) \hat{\psi}(0) \rangle = \exp(-\frac{\hbar^2 r^2}{2m})$ . Then, for the single-particle correlation function we obtain:

$$g_1(r) = \langle \hat{\psi}^\dagger(r) \hat{\psi}(0) \rangle = n \exp \left\{ -\frac{1}{2} \langle (\hat{\phi}_p(0) - \hat{\phi}_p(r))^2 \rangle \right\}; \quad T \approx T_d; \quad (2.52)$$



In the 2D case, vacuum low-energy (long-wave) fluctuations of the phase are small as  $m g = 2 \sim^2$ . However, thermal phase fluctuations are large for  $r \ll 1$ . On the basis of Eq.(2.47), we find the following asymptotic expression for the mean square phase fluctuations:

$$\langle \hat{\phi}_p(r) \rangle^2 = \langle \hat{\phi}_p(0) \rangle^2 + \frac{2T}{T_d} \ln \frac{r}{T} ; \quad r \gg T : \quad (2.53)$$

where  $T$  is equal to the healing length  $\xi_c$  at  $T = T_d$ , and to the thermal de Broglie wavelength of phonons  $\lambda_{cs} = T$  for  $T < T_d$ . Accordingly, the correlation function  $g_1(r)$  undergoes a slow power law decay at large distances:

$$g_1(r) = n \frac{T}{r} \quad ; \quad r \gg T : \quad (2.54)$$

This is drastically different from the situation in 3D Bose-condensed gases, where fluctuations are small at any distance and  $g_1$  is tending to the condensate density as  $r \ll 1$ . We thus see that just long-wave thermal fluctuations of the phase destroy the long-range order and true BEC in finite-temperature 2D Bose gases.

The low-temperature behavior of the single-particle correlation function, showing its power law decay at large  $r$ , was first obtained by Kane and Kadano [9]. The idea of dividing the system into slow (low-energy) and fast (high-energy) parts belongs to Popov who developed a perturbation theory for Bose systems on these grounds [1]. In the described hydrodynamic approach, for obtaining perturbative corrections to Eq.(2.52) one should expand the continuity and Euler equations (2.41) and (2.42) up to second order in the density and phase fluctuations, which provides a correction to the stationary solution. One should then include the low-energy density fluctuations and the high-energy fluctuations in the expression for the field operator. An expression for  $g_1(r)$  in the uniform 2D case, which contains these corrections and is obtained on the basis of the Popov theory, is given in [35].

The distance at which the mean square phase fluctuations become of the order of unity and the single-particle correlation function significantly decreases, is called the phase coherence length  $l$ . From Eq.(2.53) we obtain

$$l = T \exp \frac{T_d}{2T} \quad (2.55)$$

and clearly see that at  $T = T_d$  the phase coherence length greatly exceeds the healing length  $\xi_c$ . This means that the system can be divided into blocks of size  $L$  which is chosen such that  $\xi_c \ll L \ll l$ . Then, using Eqs. (2.52) and (2.53) we can make sure that correlation properties inside each block are the same as in a genuine Bose-condensed gas. We thus conclude that there is a true condensate in each block. However, the phases of different blocks are not correlated with each other. Therefore, this system got the term quasicondensate, or condensate with fluctuating phase [13]. For the existence of the quasicondensate, it is crucial that the density fluctuations are small on any distance scale.

## 2.5 True and quasicondensates in 2D traps

Bose-Einstein condensation in trapped 2D gases is qualitatively different from that in the uniform case. As was discussed in Lecture 1, for an ideal 2D gas the change of the density of states due to a harmonic confining potential, leads to a macroscopic occupation of the ground state of the trap (ordinary BEC) at temperatures  $T < T_c = N^{1/2} \sim 1$ , where  $N$  is the number of particles, and  $1$  the trap frequency [7]. Thus, there is a question of whether an interacting

trapped 2D gas supports the ordinary BEC or the Kosterlitz-Thouless type of a cross-over to the BEC regime. Related studies are now underway, and for large 2D samples one expects the Kosterlitz-Thouless cross-over. However, irrespective of the type of the BEC cross-over, the critical temperature will be always comparable with  $T_c$  of an ideal gas. On approach to  $T_c$  from above, the gas density is  $n_c = N/R_{T_c}^2$ , where  $R_{T_c} = \lambda_{T_c}^2$  is the thermal size of the cloud, and hence the Kosterlitz-Thouless temperature is  $n_c \sim N^{1/2} \sim 1/\lambda_{T_c}^2$ .

An important feature of trapped gases is that the confining potential introduces a finite size of the sample, which sets a lower bound for the momentum of elementary excitations and reduces the phase fluctuations. For this reason, at finite temperatures well below  $T_c$  the phase fluctuations are small, and the equilibrium state is a true condensate. At intermediate temperatures  $T < T_c$  the phase fluctuates on a distance scale smaller than the size of the gas sample, and one has a quasicondensate. Qualitatively, the character of the BEC state can be identified by comparing the size of the sample with the uniform-gas phase coherence length (2.55) at the maximum density of the trapped gas. In this Lecture we present a more detailed analysis of the phase fluctuations and BEC character in weakly interacting trapped (quasi)2D gases. For simplicity we assume that the coupling constant  $g$  is independent of the gas density. In the quasi2D case this requires the condition  $\hbar^2 \omega_i \gg \mu$  which leads to  $g$  given by Eq.(2.8). This condition is satisfied in recent experiments [16{19], where the quasi2D regime was reached for atomic Bose condensates.

For finding the phase (and density) fluctuations in a trapped gas, one should know the density profile and the spectrum of elementary excitations. If the number of particles is very large and the chemical potential greatly exceeds the level spacing in the trap, the kinetic energy term in Eq. (2.43) is much smaller than the nonlinear term and can be neglected. This approach is called the Thomas-Fermi (TF) approximation, and in a harmonic trap the density profile takes the well-known parabolic shape:

$$n = \frac{1}{g} \sum_i \frac{m}{2} \omega_i^2 r_i^2; \quad (2.56)$$

with  $\omega_i$  and  $r_i$  being the trap frequency and coordinate in the  $i$ -th direction. The dependence of the excitation spectrum on the trapping geometry has been extensively studied for 3D TF condensates (see [39] for review). The spectrum and wavefunctions of low-energy excitations ("phonons") can be found analytically [36{38]. For the 1D and 2D weakly interacting trapped Bose gases this has been done in [40,41].

We analyze the character of BEC in a harmonically trapped symmetric 2D gas with repulsive interparticle interaction, relying on the calculation of the single-particle correlation function [20]. As well as in the uniform case, fluctuations of the density are provided by excitations with wavelengths of the order of  $\lambda_c$  and in a similar way one proves that they are small at temperatures  $T \ll T_d$ . Therefore, the single-particle correlation function can be found by using the field operator from Eq.(2.51), with coordinate-dependent mean density  $n(r)$  and phase operator  $\hat{\varphi}(r)$ . Then the correlation function is given by Eq.(2.52) generalized to the trapped case:

$$\langle \hat{\psi}^\dagger(r) \hat{\psi}(0) \rangle = \frac{1}{n_0(r)n_0(0)} \exp \left[ \frac{i}{2} \langle (\hat{\varphi}_p(0) - \hat{\varphi}_p(r))^2 \rangle \right]; \quad (2.57)$$

where  $r = 0$  at the trap center.

In the Thomas-Fermi regime, the radius of the gas sample is  $R_{TF} = (2\mu/m\omega^2)^{1/2}$ , and integration of Eq.(2.56) over the spatial volume of the gas gives a relation between the chemical

potential and the number of particles:

$$= n_0 m g = \frac{r}{\lambda^2} \frac{N m g}{2} \sim ! ; \quad (2.58)$$

where  $n_m = n(0)$  is the maximum density. It is worth noting that the ratio of the chemical potential to the BEC transition temperature  $T_c$  of an ideal gas is  $\mu/T_c = (m g / \lambda^2)^{1/2} \approx 1$ .

For calculating the mean square fluctuations of the phase, we use the (discrete) spectrum and wavefunctions of excitations with energies  $\epsilon_p$ , obtained relying on the method developed for Thomas-Fermi trapped condensates [36, 38, 40, 41]. At temperatures larger than the chemical potential, for distances  $r$  greatly exceeding the healing length  $\lambda_c$  at the trap center, we obtain a result similar to that in the uniform case:

$$\langle \hat{\psi}_p(0) \hat{\psi}_p(r) \rangle^2 \approx \langle \hat{\psi}_p(r) \rangle^2 \approx \frac{m g}{\lambda^2} \frac{T}{2} \ln \frac{r}{\lambda_c} ; \quad (2.59)$$

The character of the Bose-condensed state is determined by the phase fluctuations at distances  $r \approx R_{TF}$ . If they are small, one has a true condensate, and for a large value of these fluctuations the state is a quasicondensate. With logarithmic accuracy, from Eq.(2.59) we find

$$\langle \hat{\psi}_p(r \approx R_{TF}) \rangle^2 \approx \frac{m g}{2 \lambda^2} \frac{T}{2} \ln N ; \quad (2.60)$$

In the case of a quasicondensate the phase coherence length  $l$  is given by an expression similar to that for uniform quasicondensates. For  $T > T_c$ , equation (2.59) yields  $l \approx \lambda_c \exp(-\mu/n_m T)$ . As  $l$  greatly exceeds the healing length, the quasicondensate has the same Thomas-Fermi density profile as the true condensate. Correlation properties at distances smaller than  $l$  and, in particular, local density correlators are also the same. Hence, one expects the same reduction of inelastic decay rates as in 3D condensates [13]. However, the phase coherence properties of a quasicondensate are drastically different. We will have a detailed discussion of this subject in the next Lecture for the case of 1D quasicondensates.

From Eq.(2.60) we see that in large gas samples one has more possibilities for obtaining the quasicondensate regime. In quasi2D trapped alkali gases one can expect the number of trapped atoms  $N$  ranging from  $10^4$  to  $10^6$  and a value  $\lambda \approx 10^{-2}$  or larger for the small parameter  $g \approx 2 \lambda^{-2}$ . In the MIT sodium experiment [16] on achieving the quasi2D regime for a trapped condensate, this small parameter was about  $10^{-2}$  and the number of atoms was  $10^6$ . Therefore, even at temperatures somewhat higher than  $T_c$  the gas was in the regime of true BEC. Note, however, that the coupling constant  $g$  in the MIT experiment [16] was rather small as the scattering length for sodium is only 28 Å. One can think of achieving the quasicondensate regime for the same trapping parameters and  $N$  as at MIT, by using Feshbach resonances and tuning the coupling constant to much larger values.

Presently, the largest obtained 2D Bose-condensed gas is the one of spin-polarized atomic hydrogen on liquid helium surface [15]. In this system the temperature is about 100 mK, the density exceeds  $10^{13} \text{ cm}^{-3}$ , and the number of particles is  $10^8$ . Estimates show that the state should be a quasicondensate rather than a true condensate. However, this should still be proven experimentally.

**Problem:** Prove that to zero order in perturbation theory the coupling constant for the 2D Bose-condensed gas is  $g = \lambda^2 f m$ , where  $f$  is the scattering amplitude (as defined in Eq.(2.13)) at energy of the relative motion  $E = 2 \mu$ . (Yu.E. Lozovik, 1971).

## 3 LECTURE 3. TRUE AND QUASICONDENSATES IN 1D TRAPPED GASES

One-dimensional Bose systems at low temperature show a remarkable physics not encountered in 2D and 3D. In particular, the 1D Bose gas with repulsive interparticle interaction becomes more non-ideal with decreasing 1D density  $n$  [42,43]. The regime of a weakly interacting gas requires the correlation length  $\xi_c = \sqrt{\frac{\hbar^2}{m n g}}$  to be much larger than the mean interparticle separation  $1/n$ . For small  $n$  or large interaction, where this condition is violated, the gas acquires fermionic properties as the wavefunction strongly decreases at short interparticle distances [42,43]. In this case it is called a gas of impenetrable bosons or Tonks-Girardeau gas (cf. [44]).

Spatially uniform 1D Bose gases with repulsive interparticle interaction have been extensively studied in the last decades. For the delta-functional interaction, Lieb and Liniger [43] have calculated the ground state energy and the excitation spectrum which at low momenta turns out to be phonon-like. Generalizing the Lieb-Liniger approach, Yang and Yang [45] have proved the analyticity of thermodynamic functions at any finite temperature  $T$ , which indicates the absence of a phase transition.

However, at sufficiently low  $T$  the correlation properties of a 1D Bose gas are qualitatively different from classical high- $T$  properties. In the regime of a weakly interacting gas the density fluctuations are suppressed [9], whereas at finite  $T$  the long-wave fluctuations of the phase lead to an exponential decay of the single-particle correlation function at large distances [9,46]. A similar picture, with a power-law decay of the density matrix, was found at  $T = 0$  [47,48]. Therefore, the Bose-Einstein condensate is absent at any  $T$ , including  $T = 0$ . These findings are consistent with the Bogoliubov  $k^{-2}$  theorem at finite  $T$ , and with a related treatment at  $T = 0$  [49].

Earlier studies of 1D Bose systems (see [1] for review) allow us to conclude that in uniform 1D gases the decrease of temperature leads to a continuous transformation of correlation properties from ideal-gas classical to interaction/statistics dominated. In the weakly interacting regime at low  $T$ , where the density fluctuations are suppressed and the phase fluctuates on a distance scale much larger than the correlation length  $\xi_c$ , one can speak of a phase-fluctuating Bose-condensed state (quasicondensate). A 1D classical field model for calculating correlation functions in the conditions, where both the density and phase fluctuations are important, was developed in [50] and for Bose gases in [51]. The use of the Bogoliubov approach for describing 1D uniform (quasi)condensates is recently discussed in [52] and is presented in the lectures of Yvan Castin.

In order to avoid misunderstanding, we should make a remark on the presence of a quasicondensate in the uniform weakly interacting 1D Bose gas. It is sometimes stated that in this case the quasicondensate exists only at  $T = 0$ , and its presence is related to the power law decay of the single-particle correlation function at large distances (see, for example, [53]). However, at finite temperatures where this correlation function decays exponentially, the phase coherence length  $l$  can greatly exceed the healing length  $\xi_c$ . This is the case for small density fluctuations, and then the physical picture is similar to that in uniform finite-temperature 2D gases or zero-temperature 1D gases. The system can be divided into blocks of size  $L$  satisfying the inequalities  $\xi_c \ll L \ll l$ , and inside each block one has a true condensate with a phase that is not correlated with phases in other blocks. In this sense, the term quasicondensate can also be used in weakly interacting uniform 1D Bose gases at finite temperatures.

The 1D regime for trapped atomic condensates has been achieved in several experiments by tightly confining the motion of particles in two directions [16,54,55]. In this Lecture we will discuss the various quantum degenerate states that are present in finite-temperature 1D trapped Bose gases and focus attention on the case of a weakly interacting gas.

### 3.1 Weakly interacting regime in 1D

We will discuss 1D Bose gases with repulsive short-range interaction between particles (coupling constant  $g > 0$ ). Present realizations of the 1D regime imply particles in a cylindrical trap, which are tightly confined in the radial direction, with the confinement frequency  $\omega_0$  greatly exceeding the mean-field interaction. Then, at sufficiently low  $T$  the radial motion of particles is essentially "frozen" and is governed by the ground-state wavefunction of the radial harmonic oscillator. If the radial extension of the wavefunction,  $l_0 = (\hbar/m\omega_0)^{1/2}$ , is much larger than the radius of the interatomic potential  $R_e$ , the interaction between particles acquires a 3D character and is characterized by the 3D scattering length  $a$ . For this case, the coupling constant has been found by Olshanii [56], and for  $l_0 \gg a$  it can also be obtained by averaging the 3D interaction over the radial (harmonic oscillator) density profile:

$$g = \frac{2\pi^2}{m} \frac{a}{l_0^2} ; \quad l_0 \gg a : \quad (3.1)$$

Statistical properties of such quasi-1D samples are the same as those of a purely 1D system with the coupling constant given by Eq.(3.1).

As well as in the 2D case, we obtain the criterion of the weakly interacting regime at  $T = 0$  by comparing the interaction energy per particle,  $I = ng$ , with a characteristic kinetic energy of particles at a mean separation  $r$  between them. In the 1D case we have  $r \sim 1/n$ , and this kinetic energy is  $K \sim \hbar^2 n^2/m$ . In the weakly interacting regime, where the wavefunction of particles is not influenced by the interaction at interparticle distances of the order of  $r$ , one should have  $I \ll K$ . This leads to the criterion of the weakly interacting regime

$$= \frac{mg}{\hbar^2 n} \ll 1 : \quad (3.2)$$

From Eq.(3.2) one really sees that in contrast to 2D and 3D gases, the 1D Bose gas becomes more interacting with decreasing density. In the purely 1D case this statement is valid as long as the mean interparticle separation  $1/n$  remains much larger than the radius of interparticle interaction  $R_e$ . For quasi-1D weakly interacting gases realized in present experiments, the density should still be such that the healing length  $\xi = \hbar^2/mng \gg l_0$ , otherwise the gas leaves the 1D regime. Assuming  $a \ll l_0$ , this gives the condition  $n \ll 1$ .

The parameter  $\xi$  can also be interpreted as a ratio of the mean interparticle separation to the characteristic interaction length for two particles,  $r_g = \hbar^2/mg$ . This quantity determines the distance scale on which the repulsion between the particles reduces their relative wavefunction. Under the condition  $r_g \gg 1/n$ , which is equivalent to Eq.(3.2), this reduction is practically absent and, hence, the gas is weakly interacting. In contrast, for  $r_g \sim 1/n$  or, equivalently,

$1$ , the relative wavefunction is strongly reduced at distances smaller than  $1/n$ . The gas then enters the strongly interacting Tonks-Girardeau regime and acquires fermionic properties.

For particles trapped in a harmonic (axial) potential  $V(z) = m\omega_0^2 z^2/2$ , one can introduce a complementary dimensionless quantity

$$= \frac{mg l}{\hbar^2} ; \quad (3.3)$$

where  $l = \hbar/m\omega_0$  is the amplitude of axial zero point oscillations. The parameter  $\xi$  provides a relation between the interaction strength  $g$  and the trap frequency  $\omega_0$ . Actually, it represents the ratio of  $l$  to the interaction length  $r_g$ . For  $\xi \gg 1$ , the strongly interacting regime is not present at all as the relative motion of two particles on approach to each other is governed by their harmonic confinement rather than the interparticle interaction.

### 3.2 True BEC and diagram of states at $T = 0$

The nature of quantum degenerate states in the trapped 1D gas is strongly influenced by the interparticle interaction and by the presence of the trapping potential. The latter introduces a finite size of the sample and provides a low-momentum cut-off for the phase and density fluctuations. This reduces the fluctuations compared to the uniform case.

We first discuss the case of  $T = 0$ . For simplicity, we will consider a uniform gas with a finite size  $L$ . We assume a priori that there is a true condensate with a density  $n_0$  greatly exceeding the density of non-condensed particles  $n^0$ . Then, for a large value of  $L$  we have the Bogoliubov excitation spectrum given by Eq.(2.33) and the excitation wavefunctions following from Eq.(2.32). The density of non-condensed particles is given by an equation similar to Eq.(2.34). The difference is that now the lower limit of integration over the excitation momenta is non-zero. It is related to a finite size of the system and is equal to  $\pi/L$ . We thus have

$$\frac{n^0}{n_0} = \frac{1}{L} \int_{\pi/L}^{\infty} \frac{dk}{2\pi} \frac{v_k^2}{n_0} ; \quad (3.4)$$

and a straightforward calculation yields

$$\frac{n^0}{n_0} = \frac{1}{2} \ln \frac{2L}{\pi} : \quad (3.5)$$

For a realistic size  $L$  of a trapped 1D Bose gas, the logarithmic factor in Eq.(3.5) does not exceed 10. Hence, for  $L \gg 1$  we have  $n^0 \ll n_0$ . This proves that fluctuations are small and justifies our initial assumption on the presence of a true BEC in a weakly interacting trapped Bose gas at  $T = 0$ . An analysis of vacuum fluctuations for 1D Bose gases in harmonic traps is given in [41].

Thus, in a harmonically trapped 1D Bose gas at  $T = 0$  we have a true condensate with the density profile determined by the Gross-Pitaevskii equation (2.25). In the Thomas-Fermi (TF) regime, where the chemical potential is  $\mu \gg 1$ , the kinetic energy term can be omitted and we have a parabolic density distribution typical for condensates in harmonic traps:

$$n_0(z) = n_{0m} \left( 1 - \frac{z^2}{R_{TF}^2} \right) \quad (3.6)$$

for  $|z| \leq R_{TF}$ , and is equal to zero otherwise. The (half) size of the condensate is  $R_{TF} = (2\mu)^{1/2}$ , and the maximum density is  $n_0(0) = n_{0m} = \mu/g$ . Integrating Eq.(3.6) over  $dz$  we obtain a relation between the chemical potential and the number of particles  $N$ :

$$\mu = \frac{3N}{4} \frac{1}{L} \quad (3.7)$$

where the parameter  $L$  is given by Eq.(3.3).

For  $L \gg 1$  we are always in the TF regime. In this case, Eq.(3.2) requires a sufficiently large number of particles:

$$N \gg \frac{1}{L} \quad (3.8)$$

which reflects the fact that the weakly interacting regime requires sufficiently large densities. For  $L \gg 1$  the criterion (3.2) of a weakly interacting gas is satisfied at any  $N$ . The condensate is in the TF regime if  $N \gg 1$ . In the opposite limit the mean-field interaction is much smaller than the level spacing in the trap  $\sim 1/L$ . Hence, one has a macroscopic occupation of the ground state of the trap, i.e. there is an ideal gas condensate with a Gaussian density profile.

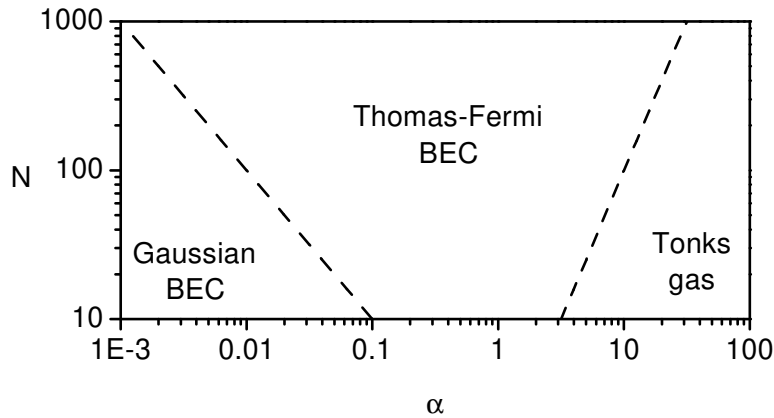


Fig. 5. Diagram of states for a trapped 1D gas at  $T = 0$ .

If  $\alpha \ll 1$  and  $N \ll N_c$ , then the trapped 1D gas is in the strongly interacting Tonks-Girardeau regime. The one-to-one mapping of this system to a gas of free fermions [42] ensures the fermionic spectrum and density profile. The chemical potential is equal to  $N^{-1}$ , and the density distribution is  $n(z) = (2N+1)^{-1} (z/R)^2$ , where the size of the cloud is  $R = \sqrt{2N+1}$ . Note that this profile is different from both the profile of the zero-temperature condensate and the classical distribution of particles. Correlation properties of strongly interacting 1D Bose gases will be discussed in Lecture 4.

In Fig. 5, we present the diagram of states for the zero-temperature trapped 1D Bose gas in terms of  $N$  and  $\alpha$ . This diagram clearly shows the presence of three states as discussed above: Thomas-Fermi BEC, condensate with a Gaussian density profile, and the Tonks-Girardeau gas.

### 3.3 Regimes of quantum degeneracy at finite temperature

The characteristic temperature of quantum degeneracy for a trapped 1D Bose gas is  $T_d \propto N^{-1}$ . In the weakly interacting regime, the character of finite-temperature Bose-condensed states at  $T \ll T_d$  is determined by thermal fluctuations. Before describing these states, we briefly analyze a cross-over to the BEC regime in 1D trapped gases.

As we discussed in Lecture 1, for an ideal gas one has a sharp cross-over to BEC. Ketterle and van Druten [8] found that the decrease of  $T$  to below  $T_c = N^{-1} \ln(2N)$  strongly increases the population of the ground state, which rapidly becomes macroscopic. This sharp cross-over originates from the discrete structure of the trap levels. However, the presence of the interparticle interaction changes the picture drastically. One can distinguish between the (lowest) trap levels only if the interaction between particles occupying a particular level is much smaller than the level spacing. Otherwise the interparticle interaction smears out the discrete structure of the levels. For  $T$  close to  $T_c$  the occupation of the ground state is  $T_c \propto N^{-1} \ln(2N)$  [8] and, hence, the mean-field interaction between the particles in this state (per particle) is  $N g \ln(2N)$ . The sharp BEC cross-over requires this quantity to be much smaller than  $N^{-1}$ , and we arrive at the condition  $N \ln(2N) \ll 1$ . For a realistic number of particles ( $N \approx 10^3 - 10^4$ ) this is practically equivalent to the condition  $N \ll 1$  at which one has the ideal gas Gaussian condensate.

As we see, the sharp BEC cross-over requires small  $\alpha$ . For possible realizations of 1D gases, using the coupling constant (3.1) for  $l_0 \approx a$ , we obtain  $\alpha = 2al_0^2$ . Then, even for the ratio  $l/l_0 \approx 10$  and moderate radial confinement with  $l_0 \approx 1 \text{ nm}$ , we have  $\alpha \approx 0.1$  for Rb atoms

(a = 50 Å). Clearly, for a reasonably large number of particles the (sharp) cross-over condition  $N^{-1}$  can only be fulfilled at extremely small interparticle interaction. One can think of reducing  $a$  to below 1 Å and achieving  $< 10^{-3}$  by using Feshbach resonances. In this case one can expect the sharp BEC cross-over already for  $N \sim 10^3$ .

Otherwise, similarly to the uniform 1D case, the decrease of temperature to below  $T_d$  continuously transforms a classical 1D gas to the regime of quantum degeneracy. If the condition (3.2) is satisfied, one has a weakly interacting gas which at  $T = 0$  becomes a true TF condensate. To understand the nature of a Bose-condensed state at finite  $T < T_d$ , we analyze the behavior of the single-particle correlation function by calculating the fluctuations of the density and phase [57].

We assume a priori that the weakly interacting trapped 1D Bose gas is characterized by small density fluctuations and justify this assumption later. Then the operators of the density and phase fluctuations are given by Eqs. (2.48) and (2.49), and the spectrum and wavefunctions of elementary excitations follow from Eqs. (2.30) and (2.31) in which the density distribution is the one of the zero-temperature condensate. It has already been shown in section 3.2 that vacuum fluctuations of the density and phase are small. Therefore, we now discuss only thermal fluctuations. Using Eq. (3.7) we find that  $\langle \delta n^2 \rangle = (2\pi N)^{1/3} \sim 1$ . Accordingly, our analysis will include both cases,  $T < T_d$  and  $T > T_d$ .

Fluctuations coming from the high-energy part of the excitations ( $j > j_0$ ) are small. Similarly to the uniform case discussed in Lecture 2, this part can be viewed as an ideal thermal gas of particles, with chemical potential equal to  $\mu = 0$ . One then finds that the number of particles in the high-energy part becomes exponentially small for  $T < T_d$ , and for  $T > T_d$  it is  $\sim (T/T_d)N \ll N$ . We therefore confine ourselves to fluctuations coming from low-energy excitations ( $j < j_0$ ).

The solution of Eqs. (2.30) and (2.31) for these excitations gives the spectrum  $\epsilon_j = \hbar^2 j(j+1) / (4mR_{TF}^2)$  [40,41] and wavefunctions

$$f_j = \frac{j+1/2}{R_{TF}} \frac{2}{j} (1-x^2)^{1/2} P_j(x) ; \quad (3.9)$$

where  $j$  is a positive integer,  $P_j$  are Legendre polynomials, and  $x = z/R_{TF}$ . Using Eqs. (2.48) and (3.9), for the mean square (thermal) fluctuations of the density we have

$$\langle \delta n^2(z) \rangle = \langle \delta n^2 \rangle_{TF} = \hbar^2 n_{0m}^2 = \sum_{j=1}^{\infty} \frac{n_{0m} j(j+1/2)}{R_{TF}} (P_j(x) - P_j(x^0))^2 N_j ; \quad (3.10)$$

with  $N_j = [\exp(\epsilon_j/kT) + 1]^{-1}$  being the occupation numbers for the excitations. Assuming  $T \sim T_d$ , the main contribution to the density fluctuations comes from quasiclassical excitations ( $j \gg 1$ ). These fluctuations are largest on a distance scale  $\lambda_j \sim \lambda_{dB}^2/j$  greatly exceeding the de Broglie wavelength of the excitations. In this case we obtain

$$\frac{\hbar^2 n_{0m}^2}{n_{0m}^2} = \frac{T}{T_d} m \ln(T/T_d) ; \quad (3.11)$$

Thus, we see that the density fluctuations are small at any temperature  $T < T_d$ .

The result of Eq. (3.11) looks quite different from what one finds for a uniform 1D Bose gas. In the latter case, using the Bogoliubov spectrum (2.33) and excitations wavefunctions (2.32), for  $T > T_d$  we have  $\hbar^2 n_{0m}^2 / (T - T_d) n^2$ . The difference from Eq. (3.11) is related to the fact that in the trapped case the density profile shrinks when decreasing temperature well below the



global temperature of quantum degeneracy  $T_d = N^{-1}$ . Therefore, at  $T = T_d$  the local value of the degeneracy temperature in the center of the trap is  $T_0 = 2^{-2} n_{0m}^2 = T_d^2 = T_d$ . Expressing  $T_d$  in Eq.(3.11) through  $T_0$  we restore qualitatively the uniform-gas result.

As the low-energy fluctuations of the density are suppressed and high-energy fluctuations are also small, for finding the single-particle correlation function we may use the field operator in the form (2.51):  $\hat{\psi}(z) = \sqrt{n_0(z)} \exp(i\hat{\phi}_p(z))$ , where the operator  $\hat{\phi}_p$  represents the low-energy part of the phase fluctuations. Then, similarly to the 2D case, the correlation function is expressed through the mean square fluctuations of the phase:

$$g_1(z; z^0) = \langle \hat{\psi}^\dagger(z^0) \hat{\psi}(z) \rangle = \sqrt{n_0(z)n_0(z^0)} \exp\left(-\frac{1}{2} \langle \hat{\phi}_{zz^0}^2 \rangle\right); \quad (3.12)$$

where  $\hat{\phi}_{zz^0}^2 = \langle \hat{\phi}_p^2(z) + \hat{\phi}_p^2(z^0) \rangle$ . On the basis of Eqs. (2.49) and (2.30), for the thermal phase fluctuations we have

$$\langle \hat{\phi}_{zz^0}^2 \rangle_T = \sum_{j=1}^{\infty} \frac{(j+1/2)}{j n_{0m} R_{TF}} \langle P_j(x) - P_j(x^0) \rangle^2 N_j; \quad (3.13)$$

In contrast to the 2D gas, thermal fluctuations of the phase in 1D are mostly provided by the contribution of the lowest excitations. A direct calculation of Eq.(3.13) yields

$$\langle \hat{\phi}_{zz^0}^2 \rangle_T = \frac{4T}{3T_d} \ln \frac{(1-x^0)(1+x)}{(1+x^0)(1-x)}; \quad (3.14)$$

For  $z$  and  $z^0$  close to the trap center, the logarithmic term in Eq.(3.14) is equal to  $2\ln z^0/R_{TF} \approx 1$ . Otherwise, it is of order unity, except for the region close to the Thomas-Fermi border of the density distribution.

The temperature  $T$  at which the quantity  $\langle \hat{\phi}_{zz^0}^2 \rangle$  is of order unity on a distance scale  $z \approx z^0 \approx R_{TF}$ , is given by

$$T = T_d \frac{1}{3}; \quad (3.15)$$

Thus, for  $T = T_d$  both the density and phase fluctuations are suppressed, and there is a true condensate. The condition (3.8) always provides the ratio  $T = N^{-1} = (4N)^{-1/3} \approx 1$ .

In the temperature range, where  $T_d = T = T$ , the density fluctuations are suppressed, but the phase fluctuates on a distance scale  $l \approx R_{TF}(T = T) \approx R_{TF}$ . Hence, similarly to the 2D case, we have a condensate with fluctuating phase (quasicondensate). The phase coherence length  $l$  greatly exceeds the correlation length:  $l \approx \frac{1}{k}(T_d = T) \approx l_c$ . Therefore, the quasicondensate has the same density profile and local correlation properties as the true condensate.

In Fig. 6, we present the state diagram for the finite-temperature trapped 1D gas at  $\mu = 10$  ( $N = 100$ ). One clearly sees three quantum degenerate regimes: the BEC regimes of a quasicondensate and true condensate, and the regime of a trapped Tonks gas [57]. For  $N \gg N_c$ , the decrease of temperature to below  $T_d$  leads to the appearance of a quasicondensate which at  $T < T_d$  turns to the true condensate. In the  $T - N$  plane the approximate border line between the two BEC regimes is determined by the equation  $(T = N^{-1}) = (32N/9N_c)^{1/3}$ . For  $N < N_c$  the system can be regarded as a trapped Tonks gas.

A cross-over from one regime to another is always smooth. The absence of a sharp transition from true to quasi-BEC is seen from the behavior of the single-particle correlation function.

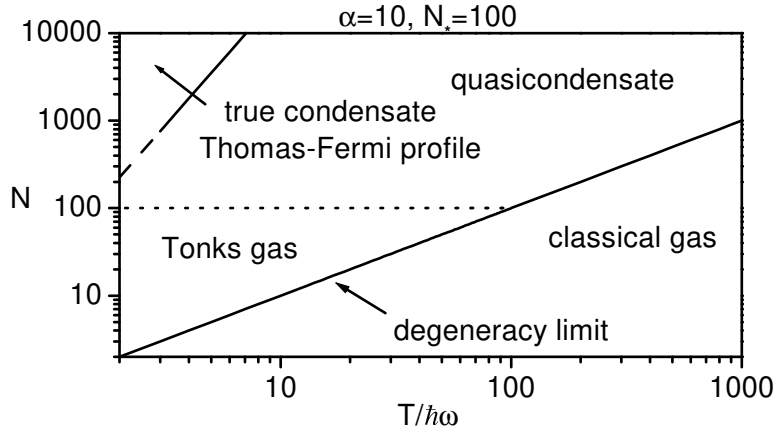


Fig. 6. D iagram of states for a finite-temperature trapped 1D Bose gas.

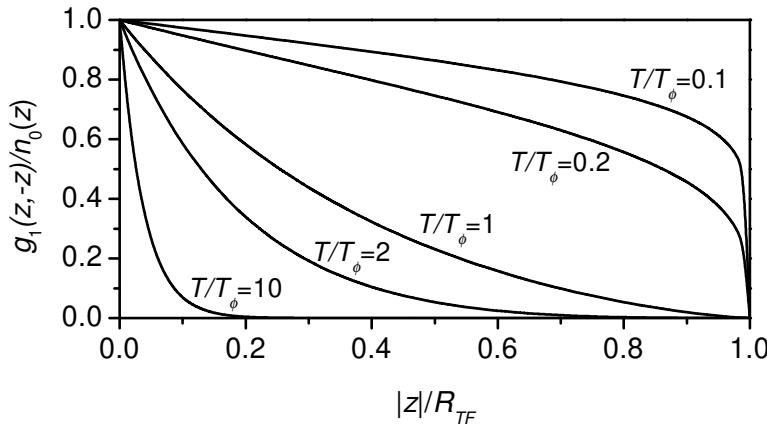


Fig. 7. Normalized single-particle correlation function  $g_1(z; -z)/n_0(z)$  versus  $|z|/R_{TF}$ .

Using Eqs. (3.12) and (3.14) and omitting small vacuum fluctuations, for the normalized correlation function at  $z^0 = -z$  we obtain

$$\frac{g_1(z; -z)}{n_0(z)} = \frac{1 - \frac{|z|}{R_{TF}} \frac{4T}{3T_\phi}}{1 + \frac{|z|}{R_{TF}}} : \quad (3.16)$$

This function is displayed in Fig. 7 for various ratios  $T/T_\phi$ . In particular, we see that the full phase coherence requires temperatures well below  $T_\phi$ .

Present facilities allow one to achieve both the true and quasicondensate regimes for the 1D trapped Bose gas. For example, in the case of  $10^3$  rubidium atoms trapped in a cylindrical harmonic potential with axial frequency  $\omega = 1$  Hz, we have the temperature of quantum degeneracy  $T_d \approx 100$  nK. Then, if the tight radial confinement providing the 1D regime is made at a frequency  $\omega_0 \approx 100$  Hz, the characteristic temperature  $T_\phi$  is about 10 nK.

The phase fluctuations lead to a drastic difference of the phase coherence properties of a quasicondensate from those of a true condensate. This can be understood from a gedanken 'juggling' experiment similar to those with 3D condensates at NIST and Munich [58,59]. Small clouds of atoms are ejected from the main cloud by stimulated Raman or RF transitions.

Observing the interference between two clouds, simultaneously ejected from different parts of the sample, allows the reconstruction of the spatial phase coherence properties. Repeatedly juggling clouds of a small volume from points  $z$  and  $z^0$  of the 1D sample, for equal time of flight to the detector we have the averaged detection signal  $I = [n_0(z) + n_0(z^0) + 2\langle \hat{h}^y(z) \hat{h}^y(z^0) \rangle]$  and thus measure directly the single-particle correlation function  $g_1(z; z^0) = \langle \hat{h}^y(z) \hat{h}^y(z^0) \rangle$ .

In the regime of a weakly interacting gas, at  $T \ll T_c$  the phase fluctuations are small and one has a true condensate. In this case, for  $z^0 = z$  we have  $\langle \hat{h}^y(z) \hat{h}^y(z^0) \rangle = n_0(z)$  and  $I = 4n_0(z)$ , which shows a pronounced interference effect. The detected signal is twice as large as the number of atoms in the ejected clouds. The phase fluctuations grow with  $T$  and for  $T > T_c$ , where the true condensate turns into a quasicondensate, the detection signal decreases as described by  $g_1(z; z)$  from Eq.(3.16). For  $T \gg T_c$  the phase fluctuations completely destroy the interference between the two ejected clouds, and  $I = 2n_0(z)$ .

The time-dependent single-particle correlation function  $\langle \hat{h}^y(z; t) \hat{h}^y(z^0; t^0) \rangle$  has been calculated in [53] and it has been shown how this correlation function can be measured in two-photon Raman outcoupling experiments.

### 3.4 Phase coherence in 3D elongated condensates

The one-dimensional character of thermal phase fluctuations is also present in a very elongated 3D Bose gas, which leads to the appearance of a quasicondensate in this system. This phenomenon, predicted [60] and observed [61{65] in recent studies, is described by the following physical picture. Excitations of elongated condensates can be divided into two groups: "low energy" axial excitations with energies  $\epsilon < \hbar \omega_0$ , and "high energy" excitations with  $\epsilon > \hbar \omega_0$ . The latter have 3D character as their wavelengths are smaller than the radial size  $R_\perp$ . Therefore, as in ordinary 3D condensates, these excitations can only provide small phase fluctuations. The "low-energy" axial excitations have wavelengths larger than  $R_\perp$  and exhibit a pronounced 1D behavior. Just these excitations give the most important contribution to the long-wave axial fluctuations of the phase.

A detailed description of fluctuations in elongated 3D condensates is given in [60], and in this Lecture we only briefly outline the results. We consider a cylindrical Thomas-Fermi condensate with an axial size  $R_{TF}$  greatly exceeding the radial size  $R_\perp$ , and assume that most particles are Bose-condensed. The axial thermal fluctuations of the phase, with wavelengths larger than  $R_\perp$ , are similar to the fluctuations in the 1D case. In particular, one finds that the mean square fluctuations on a distance scale  $R_{TF}$  are approximately equal to  $T/T_c$ , where the characteristic temperature  $T_c$  is given by

$$T_c = 15 \frac{(\hbar \omega_0)^2}{32} N^{-1/3}; \quad (3.17)$$

with  $N$  being the number of particles, and  $\omega_0$  the axial trap frequency. This is qualitatively the same as the result of Eq.(3.15) where one substitutes  $T_d = N \hbar \omega_0$ . Accordingly, the phase coherence length is again determined by the relation  $l = R_{TF} (T/T_c)$ . It is much larger than the healing length:  $l = l_c (T_c/T) (T_c/\hbar \omega_0)^2 \gg l_c$ , with  $T_c = (N \omega_0^2 / 12)^{1/3}$  being the BEC transition temperature, and  $\omega_0$  the radial confinement frequency ( $\omega_0 \gg \omega_c$ ).

We thus see that the situation is quite similar to that in 1D trapped gases. One has a continuous transformation of a quasicondensate into a true BEC when decreasing temperature to below  $T_c$ .

Most important is the dependence of the phase fluctuations on the aspect ratio of the cloud  $\omega_0/\omega_c$ . Fig. 8 shows the ratios  $T_c/T_c^0$ ,  $T/T_c$ , and the temperature  $T$  as functions of  $\omega_0/\omega_c$  for

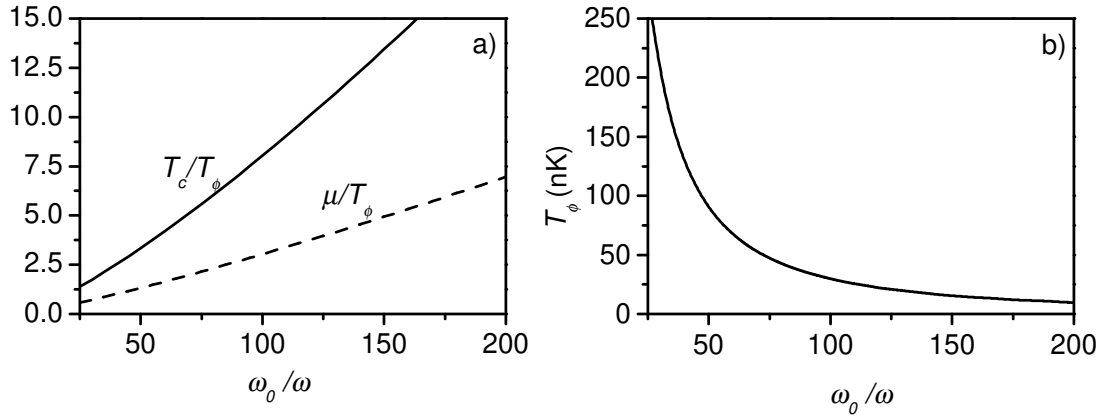


Fig. 8. The ratios  $T_c/T_0$  and  $\mu/T_0$  in (a) and the temperature  $T_0$  in (b), versus the aspect ratio  $\omega_0/\omega$  for trapped Rb condensates with  $N = 10^5$  and  $\omega_0 = 500$  Hz.

Thomas-Fermi rubidium condensates at  $N = 10^5$  and  $\omega_0 = 500$  Hz. From these results we see that 3D quasicondensates can be obtained in elongated geometries with  $\omega_0/\omega \approx 50$ .

The phase fluctuations are very sensitive to temperature. From Fig. 8 we see that one can have  $T = T_c < 0.1$ , and the phase fluctuations are still significant at  $T < 0.1$ , where only a tiny indiscernible thermal cloud is present. This suggests a principle for the formation of 3D Bose-condensed gases with indiscernible thermal clouds. If the sample is not an elongated quasicondensate by itself, it is first transformed to this state by adiabatically increasing the aspect ratio  $\omega_0/\omega$ . This does not change the ratio  $T = T_c$  as long as the condensate remains in the 3D Thomas-Fermi regime. Second, the phase coherence length  $l$  or the single-particle correlation function are measured. These quantities depend on temperature if the latter is of the order of  $T_c$  or larger. One thus can measure the ratio  $T = T_c$  for the initial cloud, which is as small as the ratio  $T = T_c$  for the elongated cloud.

Pronounced phase fluctuations have been first observed in Hannover experiments with very elongated cylindrical 3D condensates of up to  $10^5$  rubidium atoms [61, 62]. The expanding cloud released from the trap was imaged after 25 ms of time of flight and the images showed clear modulations of the density (stripes) in the axial direction (see Fig. 9). The physical reason for the appearance of stripes is the following. In a trap the density distribution does not feel the presence of the phase fluctuations, since the mean-field interparticle interaction prevents the transformation of local velocity fields provided by the phase fluctuations into modulations of the density. After switching off the trap, the cloud rapidly expands in the radial direction, whereas the axial phase fluctuations remain unaffected. As the mean-field interaction drops to almost zero, the axial velocity fields are then converted into the density distribution.

The mean square modulations of the density in the expanding cloud provide a measure of the phase fluctuations in the initial trapped condensate. A direct relation between these quantities has been established from analytical and numerical solutions of the Gross-Pitaevskii equation for the expanding cloud, with explicitly included initial fluctuations of the phase [61]. The obtained phase coherence length was inversely proportional to  $T$ , in agreement with theory, and for most measurements it was smaller than the axial size of the trapped Thomas-Fermi cloud. This implies that the measurements were performed in the regime of quasicondensation.

The properties of quasicondensates and the phase coherence length were measured directly in Bragg spectroscopy experiments with elongated rubidium BECs at Orsay [63]. In this type

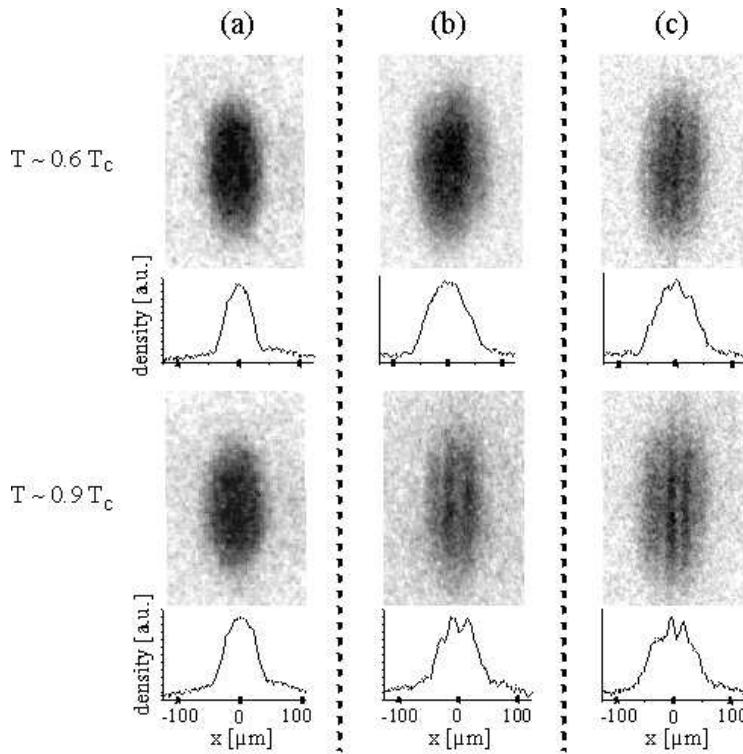


Fig. 9. Absorption images and corresponding density profiles of BECs after 25 ms time-of-flight in the Hannover experiment for aspect ratios  $l_0/l = 10$  (a), 26 (b), 51 (c).

of experiment one measures the momentum distribution of particles in the trapped gas. The Orsay studies [63] find a Lorentzian momentum distribution characteristic of quasicondensates with axially fluctuating phase [64], whereas a true condensate has a Gaussian distribution. The width of the Lorentzian momentum distribution is related to the phase coherence length at the trap center. These investigations are described in detail in the lecture of Philippe Bouyer. The phase coherence length has also been found in Hannover experiments [65] from the measurement of the intensity correlation function of two interfering spatially displaced copies of phase-fluctuating condensates.

It is important to emphasize that the measurement of phase correlations will allow one to study the evolution of phase coherence in the course of the formation of a condensate out of a non-equilibrium thermal cloud. This problem has a rich physics. For example, recent experiments on the formation kinetics of trapped condensates [66] indicate the appearance of non-equilibrium quasicondensates slowly evolving towards the equilibrium state.

**Problem :** Calculate the momentum distribution for the weakly interacting 1D Bose gas in a rectangular box of size  $L$  at temperatures much smaller than the temperature of quantum degeneracy. Describe how the momentum distribution changes when the gas transforms from the true to quasicondensate.

## 4 LECTURE 4. CORRELATIONS IN STRONGLY INTERACTING 1D BOSE GASES

In Lectures 2 and 3, we saw that the reduction of spatial dimensionality in trapped Bose gases increases the number of possible quantum degenerate states. In 3D we have (true) Bose-Einstein condensates and they were extensively studied in a large variety of experiments during last years. In the 2D case, there are two types of Bose-condensed states: true condensates and quasicondensates. In 1D, besides these BEC states, one can have a trapped Tonks gas which should exhibit some of the fermionic properties. Static and dynamical properties of strongly interacting trapped Bose gases are discussed in the lectures of Maxim Olshanii and Sandro Stringari.

In this Lecture we discuss correlation properties of strongly interacting Bose gases, which are drastically different from those in the weakly interacting regime. This is especially interesting in view of a rapid progress of experimental studies which have already reached an intermediate regime between the weakly and strongly interacting ones [67,68].

Beyond the weakly interacting regime one can no longer use the mean-field Bogoliubov approach. Nevertheless, long-wave properties are generic and can be studied relying on the quantum hydrodynamic approach developed by Haldane [48] and widely used for uniform 1D systems (see [69] for a recent overview). We will employ this approach for studying long-distance phase coherence in 1D trapped Bose gases [70].

The problem of short-range correlations requires more sophisticated approaches. The term "short-range" is used in the sense that the distance is of the order of or smaller than the characteristic correlation length of the gas, which for repulsive interaction is  $l_c = \hbar^2 / m \mu$  with  $\mu$  being the chemical potential. However, the distance is still much larger than the radius of interatomic potential,  $R_0$ . Then, in the purely 1D case such short-range correlations may be investigated by using the Lieb-Liniger model which assumes a delta-functional interaction between the atoms.

The Lieb-Liniger model for a uniform system is exactly solvable by using the Bethe Ansatz [71]. Thermodynamic functions for this model at zero and finite temperatures have been found by Lieb and Liniger [43] and by Yang and Yang [45]. On the other hand, the problem of correlation properties is far from being completely resolved, except for some correlation functions in the limiting cases of weak and strong interactions. For example, the case of infinitely strong interactions is to a certain extent equivalent to that of free fermions and the interactions play the role of Pauli principle [42]. In this limit, any correlation function of the density is given by the corresponding expression for fermions [72]. The expressions for the one-body and two-body correlations for an arbitrary interaction strength were obtained by using the Inverse Scattering Method [73]. However, closed analytical results can be found only as perturbative expansions in the limiting cases of strong and weak interactions [74-78].

We will demonstrate the use of the Lieb-Liniger model for finding local 2-body and 3-body correlations, that is the correlations at distances much smaller than the correlation length  $l_c$  [70,79,80]. These correlations are responsible for the stability of the gas with regard to intrinsic inelastic processes, such as 3-body recombination.

## 4.1 Lieb-Liniger model for trapped 1D gases

In the case of 1D trapped gases, particles undergo zero point oscillations in two (radial) tightly confined directions and there is a question to which extent one can use the 1D Lieb-Liniger model for describing the system. We will consider repulsive interaction between particles. The 1D regime is realized if the amplitude of radial zero point oscillations  $l_0 = \hbar / m \omega_0$  is much smaller than the (axial) correlation length  $l_c = \hbar^2 / m \mu$ , where  $\omega_0$  is the frequency of the

radial confinement and  $\mu$  is the chemical potential of the 1D system. This is equivalent to the condition  $\mu \sim \epsilon_0$ . One then has a 1D system of bosons interacting with each other via a short-range potential characterized by an effective coupling constant  $g > 0$ . This constant is expressed through the 3D scattering length  $a$  [56] and for  $l_0 \gg a$  is given by Eq.(3.1). Accordingly, the 1D interaction (scattering) length is  $r_g = \frac{2}{g} = a$ . In the weakly interacting regime, the chemical potential is  $\mu \approx gn$ , and the condition  $l_0 \gg a$  leads to the inequality  $na \ll 1$ . In the Tonks-Girardeau regime the correlation length  $l_c \approx 1/n$ , and one should have  $na \gg 1$ . We thus see that irrespective of the interaction strength, it is sufficient to satisfy the inequalities

$$a \ll l_0 \quad \frac{1}{n} \ll l_0 : \quad (4.1)$$

Then the 1D regime is reached and correlation properties of the system can be analyzed on the basis of the 1D Lieb-Liniger model, which in the absence of an axial trapping potential is described by the Hamiltonian

$$H = \sum_{j=1}^N \frac{p_{x_j}^2}{2m} + g \sum_{i < j} (x_i - x_j) ; \quad (4.2)$$

with  $N$  being the number of particles. From the Hamiltonian (4.2) one easily finds that the ratio of the characteristic kinetic energy of particles at the mean interparticle separation to the interaction energy per particle, is given by the parameter  $\eta = mg \approx n^2 a$  introduced in Lecture 3 in Eq.(3.2). In the strongly interacting regime we have  $\eta \gg 1$ .

At zero temperature the energy of the system  $E_0$  can be written as

$$\frac{E_0}{N} = \frac{\eta^2 n^2}{2m} e(\eta) ; \quad (4.3)$$

where  $\eta$  is given by Eq.(3.2) but is not necessarily small, and the function  $e(\eta)$  follows from the Bethe Ansatz solution found by Lieb and Liniger [43]. This function is calculated numerically for any value of  $\eta$  [43,81,82]. In the weakly interacting regime of a quasicondensate ( $\eta \ll 1$ ) we have

$$e(\eta) = \frac{4}{3} \eta^3 = \frac{4}{3} \eta^3 ; \quad \eta \ll 1 ; \quad (4.4)$$

which coincides with the result of the Bogoliubov approach. For the strongly interacting Tonks-Girardeau regime ( $\eta \gg 1$ ) the function  $e(\eta)$  is given by

$$e(\eta) = \frac{2}{3} \eta^2 \left( 1 - \frac{4}{\eta} \right) ; \quad \eta \gg 1 : \quad (4.5)$$

The expression for the chemical potential follows immediately from Eq.(4.3):

$$\mu = \frac{\partial E_0}{\partial N} = \frac{\eta^2 n^2}{2m} \left( 3e(\eta) + \frac{de(\eta)}{d\eta} \right) ; \quad (4.6)$$

Accordingly, in the weakly interacting regime ( $\eta \ll 1$ ) we have  $\mu \approx ng$ , and in the strongly interacting Tonks-Girardeau regime the chemical potential is

$$\mu = \frac{2\eta^2 n^2}{2m} \left( 1 - \frac{4}{\eta} \right) ; \quad \eta \gg 1 : \quad (4.7)$$

In the presence of an (axial) trapping potential  $V(z) = m \omega^2 z^2/2$ , one should add this potential to the Hamiltonian (4.2). Then, for an arbitrary  $\eta$  the model is no longer integrable.

However, if the chemical potential of the 1D trapped gas satisfies the inequality  $\mu_0 \sim !$ , one can use the local density approximation [81,83]. Namely, assuming local equilibrium, the density distribution is governed by the equation

$$(\mu(z)) + V(z) = \mu_0 ; \quad (4.8)$$

where the local value of the chemical potential  $\mu(z)$  follows from the solution of the Lieb-Liniger model for a uniform gas with density equal to  $n(z)$ . In other words, the local chemical potential is given by Eq.(4.6) in which  $n = n(z)$  and  $\mu = \mu_{LL}(n(z))$ .

As  $\mu(z)$  should be positive at any local density, Eq.(4.8) leads to the Thomas-Fermi density profile with a (half) size  $R_{TF} = (2\mu_0/m)^{1/2}$ . So, in the interval of distances,  $R_{TF} < z < R_{TF}$ , the density distribution is governed by Eq.(4.8), and otherwise one has  $n(z) = 0$ . The density is maximum at the trap center ( $z = 0$ ) and it smoothly decreases to zero when moving to the Thomas-Fermi border of the trapped gas. The normalization condition

$$\int_{-R_{TF}}^{R_{TF}} dz n(z) = N ;$$

gives a relation between the chemical potential  $\mu_0$  and the number of particles  $N$ .

#### 4.2 Phase coherence at zero temperature

In Lecture 3 we showed that for a realistic (axial) size of the sample, the ground state of the weakly interacting trapped 1D Bose gas ( $\mu_0 = 1$  and  $T = 0$ ) is a true Bose-Einstein condensate. The question now is how deeply one should be in the weakly interacting regime that this statement is valid. In other words, how small should be the parameter  $\mu_0$  at the trap center for having the full phase coherence of the trapped 1D gas.

We will consider a harmonically trapped 1D Bose gas in the Thomas-Fermi regime at  $T = 0$  and calculate the single-particle correlation function  $g_1(z; z^0)$  for distances  $|z - z^0|$  greatly exceeding the correlation length  $l_c$  [70]. Assuming a priori small density fluctuations at such distances, we will rely on the 1D hydrodynamic approach [48] which describes long-wave properties of the 1D fluid in terms of the density fluctuations  $\hat{n}$  and phase  $\hat{\phi}$ . Small fluctuations of the density at large distances lead to linearized continuity and Euler equations:

$$\frac{\partial \hat{n}}{\partial t} = -\frac{\partial}{\partial z} v_J(z) \frac{\partial \hat{\phi}}{\partial z} ; \quad (4.9)$$

$$\frac{\partial \hat{\phi}}{\partial t} = -\frac{1}{m} \hat{n}(z) ; \quad (4.10)$$

where the velocities  $v_J$  and  $v_N$  are given by

$$v_J = \frac{\mu_{LL}(n(z))}{m} ; \quad (4.11)$$

$$v_N = \frac{1}{m} \frac{\partial \mu_{LL}}{\partial n} \bigg|_{n=n(z)} : \quad (4.12)$$

and the ratio  $K(z) = \frac{v_J(z)}{v_N(z)}$  is the local value of the Luttinger parameter. Using commutation relations (2.40) equations (4.9) and (4.10) can be obtained as equations of motion from the quantum hydrodynamic Hamiltonian:

$$\hat{H} = \frac{1}{2} \int_{-Z}^Z dz v_N(z) (\hat{n}^2 + v_J(z) (\partial_z \hat{\phi})^2) = \sum_j \epsilon_j \hat{b}_j^\dagger \hat{b}_j ; \quad (4.13)$$



where  $\epsilon_j$  and  $\hat{b}_j$  are eigenenergies and annihilation operators of elementary excitations. Note that in the uniform case these excitations are phonons and the velocity of sound is  $c_s = \sqrt{\frac{\rho}{m n}} \frac{d\epsilon_j}{dj}$ . Similarly, for the trapped gas the local value of the sound velocity is  $c_s = \sqrt{\frac{\rho}{m n}} \frac{d\epsilon_j}{dj}$ . The Hamiltonian (4.13) is a generalization of the effective Hamiltonian of Haldane [48] to a non-uniform system.

The solution of Eqs. (4.9) and (4.10) is given by the expansion of operators  $\hat{n}$  and  $\hat{\phi}$  in eigenmodes characterized by an integer quantum number  $j > 0$ :

$$\hat{n}(z;t) = \sum_j \frac{\epsilon_j}{2 \sqrt{v_N(0)} R_{TF}} f_j(z) \hat{b}_j \exp(-i \epsilon_j t / \hbar) + \text{h.c.}; \quad (4.14)$$

$$\hat{\phi}(z;t) = \sum_j i \frac{\sqrt{v_N(0)}}{2 \epsilon_j R_{TF}} f_j(z) \hat{b}_j^\dagger \exp(-i \epsilon_j t / \hbar) + \text{h.c.}; \quad (4.15)$$

The eigenfunctions  $f_j(z)$  are normalized by the condition

$$\int_{-1}^1 dx \frac{v_N(0)}{v_N(x)} f_j(x) f_{j'}(x) = \delta_{jj'}; \quad (4.16)$$

where we have introduced a dimensionless coordinate  $x = z/R_{TF}$ . Equations (4.9) and (4.10) are then reduced to the eigenmode equation:

$$v_N(z) \frac{\partial f_j(z)}{\partial z} - v_J(z) \frac{\partial f_j(z)}{\partial z} + \frac{\epsilon_j^2}{2} f_j(z) = 0; \quad (4.17)$$

Considering  $f_j$  as a function of the reduced coordinate  $x = z/R_{TF}$ , Eq.(4.16) takes the form:

$$(1 - x^2) f_j'' + (2x - \epsilon_j) f_j' + (\epsilon_j^2 - x^2) f_j = 0; \quad (4.18)$$

The quantity  $\epsilon_j(x) = d\ln \epsilon_j / dx$  is determined by the local parameter  $\epsilon_j(z) = m g^{-1} n(z)$ . In the Tonks regime ( $\beta \rightarrow 1$ ) we have  $\epsilon_j = 2$ , and in the weakly interacting regime  $\epsilon_j = 1$ .

The coordinate dependence of  $\epsilon_j$  is smooth and we simplify Eq. (4.17) by setting  $\epsilon_j(z) = \epsilon_j(0)$ , where  $\epsilon_j(0)$  is the value of  $\epsilon_j$  at maximum density. This simplification has been recently used [83,84] to study the excitation spectrum of trapped 1D Bose gases. Then Eq. (4.17) yields the spectrum

$$\epsilon_j^2 = \epsilon_j^2(0) + (j+1/2) \epsilon_j(0); \quad (4.19)$$

and the eigenfunctions  $f_j(x)$  are expressed through Jacobipolynomials:

$$f_j(x) = \frac{\sqrt{\frac{\epsilon_j(0)}{2(j+1/2)(j+1)(j+2+1)}}}{2(j+1/2+1)} P_j^{(\epsilon_j(0))}(x); \quad (4.20)$$

where  $\epsilon_j = 1 + \epsilon_j(0)$ .

As the density fluctuations on a large distance scale are small, for the single-particle correlation function one can write

$$g_1(z; z^0) = \langle \hat{n}^\dagger(z) \hat{n}(z^0) \rangle = \sum_j \frac{1}{n(z)n(z^0)} \exp \left( \frac{1}{2} \langle \hat{\phi}(z) - \hat{\phi}(z^0) \rangle^2 \right); \quad (4.21)$$

Using Eq. (4.15) the mean square fluctuations of the phase in the exponent of Eq. (4.18) are reduced to the sum over  $j$ -dependent terms containing eigenfunctions  $f_j$  and eigenenergies  $\epsilon_j$ . For the vacuum phase fluctuations this sum is logarithmically divergent at large  $j$ , which is

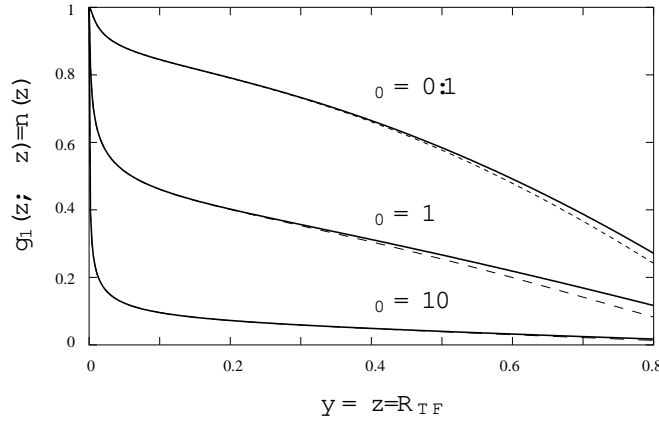


Fig. 10. Normalized single-particle correlation function  $g_1(z; z) = n(z)$  versus  $z = R_{TF}$ , for  $N = 10^4$  and various values of  $\rho_0$ . The solid curves show numerical results, and the dashed curves the results of the quasiclassical approach.

similar to the high-momentum divergence in the uniform case. Accordingly, we introduce a cut-off  $j_{\max}$  following from the condition  $j_{\max} \sim \inf(z; (z^2)g)$  and ensuring a phonon-like character of excitations at distances  $z$  and  $z^0$ . This is equivalent to having only the low-energy part of the phase fluctuations,  $\hbar(\hat{p}(z) - \hat{p}(z^0))^2$ , in the exponent of Eq.(4.18) when considering the weakly interacting regime.

The vacuum phase fluctuations have been calculated by using two approaches: numerical summation over the eigenmodes with exact  $f_j; j$  from the simplified Eq. (4.17), and quasiclassical approach assuming that the main contribution comes from excitations with  $j \ll 1$ . In the latter case, for  $z^0 = z$  we obtain

$$\hat{g}(z) = \hat{g}(z)^2 = K^{-1}(z) \ln \frac{2zj}{l_c(z)} ; \quad (4.19)$$

which is close to Haldane's result for a uniform system [48] with the Luttinger parameter  $K(z)$  and correlation length  $l_c(z)$ . In the Tonks regime we have  $K = 1$  and  $l_c = 1/n(x) = 1/n(0) - 1/(x=R_{TF})^2$ . Remarkably, in this limit the hydrodynamical expression (4.19) coincides with the recently obtained exact result [85] for the single-particle correlation function of a harmonically trapped Tonks gas.

The dependence of  $g_1$  on the dimensionless coordinate  $x$  is governed by two parameters:  $\rho_0$  and the number of particles  $N$ . In Fig. 10 we present the quantity  $g_1(z; z) = n(z)$  for  $N = 10^4$  and various values of  $\rho_0$ . As expected, the phase coherence is completely lost in the strongly interacting regime ( $\rho_0 \gg 1$ ). Moreover, on a distance scale  $z \sim R_{TF}$  the coherence is already lost for  $\rho_0 \gg 1$ , and the full phase coherence requires  $\rho_0$  well below 0.1.

#### 4.3 Local correlations at $T = 0$

The strong transverse confinement required for the 1D regime can lead to high 3D densities of a trapped gas. At a large number of particles the 3D density can exceed  $10^{15} \text{ cm}^{-3}$  and one expects a fast decay due to 3-body recombination. It is then crucial to understand how the correlation properties of the gas influence the decay rate. For this purpose, we calculate local

correlations in the 1D Bose gas and show that the decay rates are suppressed in the Tonks-Girardeau and intermediate regimes, which is promising for achieving these regimes with a large number of particles.

The rate of 3-body recombination is proportional to the local 3-particle correlation function  $g_3 = \langle \hat{\psi}^\dagger(z) \hat{\psi}^\dagger(z) \hat{\psi}^\dagger(z) \hat{\psi}(z) \hat{\psi}(z) \hat{\psi}(z) \rangle$  [86], where all field operators are taken for the same time. Similarly, the rates of 2-body inelastic processes involve the correlation function  $g_2 = \langle \hat{\psi}^\dagger(z) \hat{\psi}^\dagger(z) \hat{\psi}(z) \hat{\psi}(z) \rangle$ . Assuming that local correlation properties are insensitive to the geometry of the system we consider a uniform 1D gas of  $N$  bosons on a ring of circumference  $L$ . The gas is described by the Lieb-Liniger Hamiltonian (4.2) which we now rewrite in the second quantization:

$$\hat{H} = \int_0^L dz \left[ \frac{\hbar^2}{2m} \frac{\partial \hat{\psi}^\dagger}{\partial z} \frac{\partial \hat{\psi}}{\partial z} + \frac{g}{2} \hat{\psi}^\dagger \hat{\psi}^\dagger \hat{\psi} \hat{\psi} \right] \quad (4.20)$$

For finding  $g_2$  at  $T = 0$ , we use the Hellmann-Feynman theorem [88,89]. Namely, one shows that the expectation value of the four-operator term in the Hamiltonian (4.20) is proportional to the derivative of the ground state energy with respect to the coupling constant:

$$\frac{dE_0}{dg} = \langle \psi_0 | \frac{dH}{dg} | \psi_0 \rangle = \frac{g_2 L}{2} \quad :$$

The first identity follows from the normalization of the ground state wavefunction  $\psi_0$ , and the second one is obtained straightforwardly from the Hamiltonian (4.20). The ground state energy is given by Eq.(4.3), and for the 2-particle local correlation, we then obtain

$$g_2(\lambda) = n^2 \frac{de(\lambda)}{d\lambda} \quad : \quad (4.21)$$

In fact, the original work of Lieb and Liniger contains a similar calculation of the interaction energy.

The function  $g_2(\lambda) = n^2$  calculated by using numerical results for  $e(\lambda)$  from [82], is shown in Fig. 11. The quantum Monte Carlo calculations of  $g_2$  [87] arrive at the same results. For small and large values of  $\lambda$ , relying on Eqs. (4.4) and (4.5), we obtain:

$$\frac{g_2(\lambda)}{n^2} = 1 - \frac{2}{\lambda} \quad ; \quad \lambda \gg 1 \quad ; \quad (4.22)$$

$$\frac{g_2(\lambda)}{n^2} = \frac{4}{3} \frac{\lambda^2}{\lambda^2 + 1} \quad ; \quad \lambda \ll 1 \quad : \quad (4.23)$$

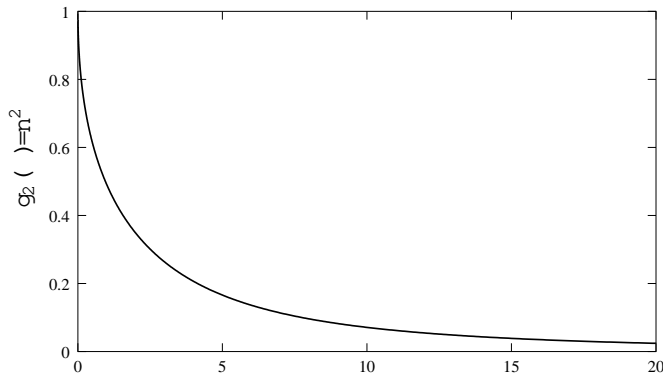
The results in Fig. 11 and Eq. (4.23) clearly show that 2-particle correlations and, hence, the rates of pair inelastic processes are suppressed for  $\lambda \gg 1$ . This provides a possibility for identifying the Tonks-Girardeau and intermediate regimes of a trapped 1D Bose gas through the measurement of photoassociation in pair interatomic collisions.

Note that for the weakly interacting regime the result of Eq.(4.22) can be obtained directly from the Bogoliubov approach. Writing the field operator in the form (2.39) and using the commutation relations (2.40), we find

$$\hat{\psi}^\dagger(z) \hat{\psi}^\dagger(z^0) \hat{\psi}(z) \hat{\psi}(z^0) = \hat{n}(z) \hat{n}(z^0) - \hat{\psi}^\dagger(z) \hat{\psi}(z^0) \quad :$$

We then represent the operator of the density as  $\hat{n}(z) = n + \delta \hat{n}(z)$  and confine ourselves to the second order in small density fluctuations  $\delta \hat{n}(z)$  around the mean density  $n$ . This gives

$$\langle \hat{\psi}^\dagger(z) \hat{\psi}^\dagger(z^0) \hat{\psi}(z) \hat{\psi}(z^0) \rangle = n^2 + \hbar \langle \delta \hat{n}(z) \delta \hat{n}(z^0) \rangle = n^2 \quad : \quad (4.24)$$

Fig. 11. Local correlation function  $g_2$  versus  $z$ .

Using the expansion of the density fluctuations in terms of Bogoliubov excitations, given by Eq.(2.46), we obtain:

$$\langle \hat{\psi}^\dagger(z) \hat{\psi}^\dagger(z^0) \hat{\psi}(z) \hat{\psi}(z^0) \rangle = n^2 + n \int_0^{\infty} \frac{dk}{2} f_k^2 (1 + 2N_k) \exp[ik(z - z^0)] ;$$

where  $E_k = \hbar^2 k^2 / 2m$ ,  $\epsilon_k = \sqrt{E_k^2 + 2E_k \mu}$  is the Bogoliubov excitation energy, and the Bogoliubov function  $f_k$  is determined by Eq.(2.32). Then, taking the limit  $z^0 \rightarrow z$  we arrive at the expression for the local 2-body correlation:

$$g_2 = \langle \hat{\psi}^\dagger(z) \hat{\psi}^\dagger(z) \hat{\psi}(z) \hat{\psi}(z) \rangle = n^2 + n \int_0^{\infty} \frac{dk}{2} \frac{E_k}{\epsilon_k} (1 + 2N_k) ; \quad (4.24)$$

For  $T = 0$  the occupation numbers for the excitations,  $N_k = 0$ , and the integration of Eq.(4.24) immediately gives the result of Eq.(4.22).

The 3-particle local correlation  $g_3$  cannot be obtained from the Hellmann-Feynman theorem. In the weakly interacting regime ( $\mu \rightarrow 0$ ) one can use the Bogoliubov approach, which gives Eq.(4.24) with an extra factor 3 in the second term of the rhs. At  $T = 0$  we then have

$$\frac{g_3(z)}{n^3} \rightarrow 1 - \frac{6\mu}{\epsilon_0} ; \quad \epsilon_0 = 0 ; \quad (4.25)$$

For the Tonks-Girardeau regime ( $\mu \rightarrow \infty$ ) we demonstrate a method for calculating the leading behavior of local correlations. Details are given in [80], and here we present a compact derivation of  $g_3$  at  $T = 0$  [70]. In the first quantization the expression for this function reads

$$g_3(z) = \frac{N!}{3!(N-3)!} \int_0^L dz_4 \dots dz_N \left( \psi_0(z_1, z_2, \dots, z_N) \right)^2 ; \quad (4.26)$$

where  $\psi_0$  is the ground state function given in the domain  $0 < z_1 < \dots < z_N < L$  by the Bethe Ansatz solution:

$$\psi_0(z_1, z_2, \dots, z_N) = \sum_P a(P) \exp \left[ i \sum_j k_{P_j} z_j \right] ; \quad (4.27)$$

where  $P$  is a permutation of  $N$  numbers, quasimomenta  $k_j$  are solutions of the Bethe Ansatz equations, and

$$a(P) = \prod_{j=1}^N \frac{i n + k_{P_j} - k_{P_1}}{i n - k_j + k_{P_1}}^{\frac{1}{2}} ;$$

For  $\eta = 1$ , we extract the leading contribution to  $\psi_0^{(1)}$  at three coinciding points by symmetrizing the amplitudes  $a(P)$  over the first three elements of the permutation  $P$ :

$$\frac{1}{3!} \sum_P a(P_{P_1}; P_{P_2}; P_{P_3}; P_4; \dots; P_N) = \frac{1}{(i n)^3} \prod_{j=1}^N (k_{P_j} - k_{P_1}) ; \quad (4.28)$$

where  $j;1=1;2;3$ . The sign of the permutation  $P$  is  $\epsilon_P$ , and  $p$  runs over six permutations of  $1;2;3$ . For large  $n$ , the difference of quasimomenta  $k_j$  from their values at  $\eta = 1$  is of order  $1/n$  and can be neglected. Then, from Eqs. (4.27) and (4.28) we conclude that to this level of accuracy the ground state wave function at three coinciding points is given by derivatives of the wave function of free fermions  $\psi_0^{(1)}(z_1; z_2; z_3; z_4; \dots)$  at  $z_1 = z_2 = z_3 = 0$ :

$$\psi_0^{(1)}(0; 0; 0; z_4; \dots) = \frac{1}{(i n)^3} \prod_{j=1}^N \left( \frac{\partial}{\partial z_j} \psi_0^{(1)} \right) ; \quad (4.29)$$

Substituting Eq. (4.29) into Eq. (4.26) we express the local correlation  $g_3$  through derivatives of the 3-body correlation function of free fermions. Using Wick's theorem the latter is given by a sum of products of 1-particle fermionic Green functions  $G(x-y) = \int_{k_F}^{\infty} dk e^{ik(x-y)} = 2\pi n$ , where  $k_F = \pi n$  is the Fermi wavevector. The calculation from Eq. (4.26) is then straightforward and in the considered limit of  $\eta = 1$  we obtain

$$\frac{g_3(\eta)}{n^3} = \frac{36}{6n^9} \langle G^0(0) \rangle^3 - \langle G^{(4)}(0) \rangle \langle G^0(0) \rangle \langle G^0(0) \rangle ; \quad (4.30)$$

which yields

$$\frac{g_3}{n^3} = \frac{16}{15} \frac{1}{n^6} ; \quad (4.31)$$

This result for  $g_3$  and the result of Eq. (4.23) for  $g_2$ , have a transparent physical explanation. A characteristic distance related to the interaction between particles is  $r_g = \lambda^2 / m g = 1/n$ , and the strong repulsion between particles provides fermionic correlations at interparticle distances  $z \sim r_g$ . For smaller  $z$  the correlation functions practically do not change. Therefore, the local correlation  $g_2$  at a finite large  $n$  is nothing else than the pair correlation function for free fermions at a distance  $r_g$ . The latter is  $g_2 = n^2 (k_F r_g)^2 = n^2$ , which agrees with the result of Eq. (4.23). Similarly,  $g_3$  is the free-fermion 3-particle correlation function at distances  $r_g$ . It is approximately equal to the product of three pair correlation functions, i.e. we have  $g_3 = n^6$  in qualitative agreement with Eq. (4.23).

Thus, from Eq. (4.31) we conclude that the 3-body decay of 1D trapped Bose gases is strongly suppressed in the Tonks-Girardeau regime. Moreover, Eq. (4.25) shows that even in the weakly interacting regime of a quasicondensate, with  $\eta = 10^{-2}$ , one has a 20% reduction of the 3-body rate. Thus, one also expects a significant reduction of the 3-body decay in the intermediate regime.

For  $l_0 \gg a$ , the 3-body recombination process in 1D trapped gases occurs at interparticle distances much smaller than  $l_0$ . Therefore, the equation for the recombination rate is the

same as in 3D cylindrical Bose-Einstein condensates with the Gaussian radial density profile  $n_{3D} = (n/l_0^2) \exp(-r^2/l_0^2)$ , where  $r$  is the radial coordinate. There is only an extra reduction by a factor of  $g_3 = n^3$ . A characteristic decay time is then given by the relation

$$\frac{n}{\tau} = g_3 \frac{1}{3D} \frac{1}{2} \frac{d}{dt} \frac{n_{3D}}{n} = \frac{3D g_3}{3(l_0^2)^2}; \quad (4.32)$$

where  $3D$  is the recombination rate constant for a 3D condensate. Even for 3D densities  $n = l_0^{-2} 10^{15} \text{ cm}^{-3}$  the life-time can greatly exceed seconds when approaching the Tonks-Girardeau regime.

In the recent rubidium experiment at NIST [68], an array of 1D tubes of bosons was created by optically confining the atoms with a radial frequency  $\omega_0 = 30 \text{ kHz}$  ( $\lambda = 350 \text{ \AA}$ ). Then, for the number of atoms  $N = 200$  in each 1D tube, the intermediate regime with  $\beta \approx 1$  has been achieved. The measurement of the 3-body decay showed a reduction of the rate by approximately a factor of seven.

#### 4.4 Finite-temperature local correlations

We now discuss local correlations in 1D Bose gases at finite temperatures and confine ourselves to two-body correlations in the uniform case [79]. The calculation of  $g_2$  will allow us to identify the various regimes of quantum degeneracy, which is important for the development of possible atom lasers in 1D waveguides. At zero temperature there are two physically distinct regimes of quantum degeneracy: the weakly interacting regime of a quasicondensate for  $\beta \ll 1$ , and the strongly interacting Tonks-Girardeau regime where the 1D gas undergoes "fermionization". These regimes are also present at finite temperatures. However, we will see that for a very small interaction strength one can have a decoherent quantum regime, where the fluctuations are enhanced and reach the non-interacting Bose gas level with  $g_2 \sim 2n^2$  (rather than  $g_2 \sim n^2$  characteristic for the quasicondensate regime). We will also see that for a large interaction strength the reduction of local correlations is present at temperatures exceeding the temperature of quantum degeneracy  $T_d = 2 \sim 2n^2/m$  and, in this respect, one has the regime of "high-temperature fermionization".

So, we again consider a 1D uniform gas of  $N$  bosons on a ring of circumference  $L$ , described by the Hamiltonian (4.2) or, equivalently, by the Hamiltonian (4.20). The exact solution of this problem at finite  $T$  has been found by Yang and Yang [45] using the Bethe Ansatz. They derived exact integral equations for thermodynamic functions and proved their analyticity. Note that in trapped gases at finite temperatures, the 1D regime requires the thermal de Broglie wavelength of particles  $\lambda_T$  to be much smaller than the amplitude of zero point oscillations in the tightly confined directions,  $l_0$ . This requirement should be added to Eq.(4.1), and we thus obtain the inequalities  $a/l_0 \ll 1$ ;  $\lambda_T \ll l_0$ . They allow us to analyze finite-temperature correlation properties of the 1D trapped gas at any  $\beta$  by using the Yang-Yang results.

The behavior of the 2-body local correlation at finite temperatures is governed by two parameters:  $\beta$  and  $\beta = 4/T = T_d$ . We first show how  $g_2$  has been calculated by using the Hellmann-Feynman theorem [88,89]. Consider the partition function  $Z = \exp(-F/T) = \text{Tr} \exp(-\hat{H}/T)$  which determines the free energy  $F$ . Here the trace is taken over the states of the system with a fixed number of particles in the canonical formalism or, for the grand canonical description, one has to replace the condition of a constant particle number by the condition of a constant chemical potential and add the term  $\mu \hat{N}$  to the Hamiltonian. For the derivative of the free energy with respect to the coupling constant one has

$$\frac{\partial F}{\partial g} = -T \frac{\partial \log Z}{\partial g} = \frac{1}{Z} \text{Tr} \frac{\partial \hat{H}}{\partial g} \exp \left( -\frac{\hat{H}}{T} \right) = \frac{g_2 L}{2}; \quad (4.33)$$

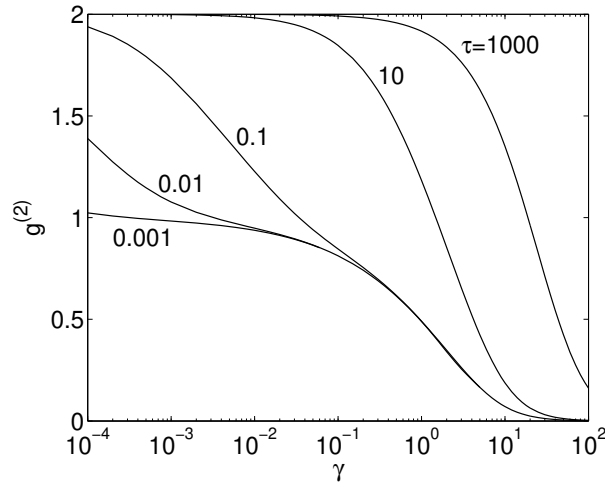


Fig. 12. Correlation function  $g^{(2)} = g_2/n^2$  versus  $\gamma$  at different  $\tau = 4/T = T_d$ .

Introducing the free energy per particle  $f(\gamma; \tau) = F/N$ , the 2-particle correlation function is:

$$g_2 = \frac{1}{n^2} \frac{\partial^2 f(\gamma; \tau)}{\partial \gamma^2} \quad (4.34)$$

In Fig. 12 we present the results for  $g_2$ , found by numerically calculating  $f(\gamma; \tau)$  from the Yang-Yang exact integral equations and then using Eq.(4.34) [79].

We now give a physical description of different regimes determined by the values of the coupling constant  $\gamma$  and the reduced temperature  $\tau$  [79]. As well as at  $T = 0$ , in the strongly interacting regime the correlation function  $g_2$  reduces dramatically due to the strong repulsion between particles, and the physics resembles that of free fermions. Interestingly, this regime is realized both below and above the quantum degeneracy temperature. Similarly to  $g_3$  and  $g_2$  at zero temperature, the finite-temperature  $g_2$  can be expressed through derivatives of the Green function of free fermions  $G(x) = \int \frac{dk}{2\pi} n_F(k) \exp(ikx) = (2\pi)^{-1} \int_{-\infty}^{\infty} dk n_F(k) \exp(ikx)$ , where  $n_F(k)$  are occupation numbers for free fermions. For the correlation function we obtain

$$\frac{g_2}{n^2} = \frac{4}{2n^4} \left( G^0(0) \right)^2 - G^0(0) G^1(0) \quad (4.35)$$

In the regime of quantum degeneracy,  $\tau \ll 1$ , the local correlation is dominated by the ground state distribution  $n_F(k) = \theta(k_F - k)$ , where  $k_F = \pi n$  is the Fermi momentum, and one only obtains a small finite-temperature correction to the zero-temperature result (4.23).

In the temperature interval  $\tau \gg 1$  the gas is non-degenerate, but the interaction length  $r_g$  is still much smaller than the thermal de Broglie wavelength  $\lambda_T$ . As well as at zero temperature,  $g_2$  can be viewed as the pair correlation function for free fermions at a distance  $r_g$ . Taking into account that the characteristic momentum of particles is now the thermal momentum  $k_T = \sqrt{2mT} \sim \pi n$ , one finds  $g_2 \sim r^2 (k_T r_g)^2 \sim r^2 = 2$ . Calculating the Green function  $G(x)$  for the classical distribution  $n_F(k)$ , we obtain:

$$\frac{g_2}{n^2} = \frac{2n^2}{2} \quad ; \quad 1 \quad ; \quad (4.35)$$

which agrees with the given qualitative estimate. The correlation function  $g_2 = n^2$  is still much smaller than unity and we thus have a regime of "high-temperature fermionization". The result of Eq. (4.35) agrees with the outcome of numerical calculations.

In the weakly interacting regime of a quasicondensate, one may use Eq. (4.24). For temperatures  $T \gg T_c$ , thermal fluctuations are more important than vacuum fluctuations, and we obtain:

$$\frac{g_2}{n^2} = 1 + \frac{1}{2} \frac{\mu}{k_B T} ; \quad \mu \ll k_B T \quad (4.36)$$

The phase coherence length is determined by thermal long-wavelength fluctuations of the phase. The calculation, similar to that for a trapped gas in Lecture 3, gives  $l_c \sim \lambda_{dB} = \sqrt{2\pi} \lambda_{dB}$ . The condition  $l_c \gg \lambda_{dB}$ , which is necessary for the existence of a quasicondensate and for the applicability of the Bogoliubov approach, immediately yields the inequality  $\mu \ll k_B T$ . Thus, Eq. (4.36) is valid under the condition  $\mu \ll k_B T$ , and the second term on the rhs of this equation is a small correction. In the region of its validity, the result of Eq. (4.36) agrees well with numerical data.

At a very weak coupling strength given by  $\mu \ll k_B T$ , the gas is in a decoherent quantum regime [51,79], where both phase and density fluctuations are large and the local correlation is always close to the result for free bosons,  $g_2 = 2n^2$ . The only consequence of quantum degeneracy is the quantum Bose distribution for occupation numbers of particles, and the decoherent quantum regime can be treated asymptotically by employing a standard perturbation theory with regard to the coupling constant  $g$ .

The presence of the quantum decoherent regime helps to explain the apparent contradiction that in the thermodynamic limit a free Bose gas at any finite temperature is known to display large thermal (Gaussian) density fluctuations with  $g_2 = 2n^2$ . For the 3D gas this result requires the grand canonical description [90], whereas in 1D and 2D it is valid for any choice of the ensemble. On the other hand, the widely used mean-field Bogoliubov approach for an interacting Bose gas leads to  $g_2 = n^2$ . The above discussed results explain this fact in the exactly solvable 1D case: there is a continuous transition from the quasicondensate to decoherent regime, depending on the density and temperature. As  $\mu$  is decreased towards a free gas, the quasicondensate result of  $g_2 = n^2$  only holds above a certain interaction strength. Below this, there is a dramatic increase in fluctuations, with  $g_2 \rightarrow 2n^2$  in the free gas limit.

**Problem:** Prove that the density fluctuations for the uniform Tonks-Girardeau gas are small in the limit of large distances. Find the distance scale on which they become large.

#### 4.5 Acknowledgements

These lectures have been given by Gora Shlyapnikov at the Les Houches summer school "Quantum Gases in Low Dimensions", organized in 2003 by Ludovic Pricoupenko, Helene Perrin, and Maxim Olshanii. Dmitry Petrov and Gora Shlyapnikov are grateful to them for support and for hospitality at Les Houches.

The authors acknowledge fruitful discussions with Carlos Lobo and Jook Walraven. The work on these lectures was financially supported by the Nederlandse Organisatie voor Wetenschappelijk Onderzoek (NWO), by the Stichting voor Fundamenteel Onderzoek der Materie (FOM), by the French Ministère de la Recherche et des Technologies, by INTAS, and by the Russian Foundation for Fundamental Research. LKB est UMR 8552 du CNRS, de l'ENS et de l'Université Pierre et Marie Curie.

#### References



- [1] V. N. Popov, *Functional Integrals in Quantum Field Theory and Statistical Physics* (D. Reidel Pub., Dordrecht, 1983).
- [2] N. D. Mermin and H. Wagner, *Phys. Rev. Lett.* **17**, 1133 (1966).
- [3] P. C. Hohenberg, *Phys. Rev.* **158**, 383 (1967).
- [4] M. H. Anderson et al., *Science* **269**, 198 (1995).
- [5] K. Davis et al., *Phys. Rev. Lett.* **75**, 3969 (1995).
- [6] C. C. Bradley et al., *Phys. Rev. Lett.* **75**, 1687 (1995).
- [7] V. Bagnato and D. Kleppner, *Phys. Rev. A* **44**, 7439 (1991).
- [8] W. Ketterle and N. J. van Druten, *Phys. Rev. A* **54**, 656 (1996).
- [9] W. Kane and L. Kadano, *Phys. Rev.* **155**, 80 (1967); *J. Math. Phys.* **6**, 1902 (1965).
- [10] V. L. Berezinskii, *Sov. Phys. JETP* **32**, 493 (1971); *ibid* **34**, 610 (1972).
- [11] J. M. Kosterlitz and D. J. Thouless, *J. Phys. C* **6**, 1181 (1973); J. M. Kosterlitz, *J. Phys. C* **7**, 1046 (1974).
- [12] N. P. Rokof'ev, O. Ruebenacker, and B. Svistunov, *Phys. Rev. Lett.* **87**, 270402 (2001); N. P. Rokof'ev and B. Svistunov, *Phys. Rev. A* **66**, 043608 (2002).
- [13] Y. Kagan, B. V. Svistunov, and G. V. Shlyapnikov, *Sov. Phys. JETP* **66**, 480 (1987).
- [14] D. J. Bishop and J. D. Reppy, *Phys. Rev. Lett.* **40**, 1727 (1978); D. J. Bishop and J. D. Reppy, *Phys. Rev. B* **22**, 5171 (1980).
- [15] A. I. Safonov et al., *Phys. Rev. Lett.* **81**, 4545 (1998).
- [16] A. G. Orłitz et al., *Phys. Rev. Lett.* **87**, 130402 (2001).
- [17] S. Burger et al., *Europhys. Lett.* **57**, 1 (2002).
- [18] D. Rychtarik, B. Engeser, H.-C. Nagel, and R. Grimm, *cond-mat/0309536*.
- [19] V. Schweikhard et al., *Phys. Rev. Lett.* **92**, 040404 (2004).
- [20] D. S. Petrov, M. Holthmann, and G. V. Shlyapnikov, *Phys. Rev. Lett.* **84**, 2551 (2000).
- [21] J. T. M. Walraven, in *Atomic Hydrogen on Liquid Helium Surfaces*, Proceedings of the Les Houches Summer School on Fundamental Systems in Quantum Optics, Session LIII, edited by J. Dalbard, J.-M. Raimond, and J. Zinn-Justin (Elsevier Science Publishers, Amsterdam, 1992).
- [22] D. S. Petrov and G. V. Shlyapnikov, *Phys. Rev. A* **64**, 012706 (2001).
- [23] L. P. Ricoupenko and M. O. Lshanii, *cond-mat/0205210*.
- [24] L. D. Landau and E. M. Lifshitz, *Quantum Mechanics, Non-relativistic Theory* (Butterworth-Heinemann, Oxford, 1999).
- [25] V. Vuletic, C. Chin, A. J. Kerman, and S. Chu, *Phys. Rev. Lett.* **81**, 5768 (1998); V. Vuletic, C. Chin, A. J. Kerman, and S. Chu, *Phys. Rev. Lett.* **83**, 943 (1999).
- [26] V. Vuletic, A. J. Kerman, C. Chin, and S. Chu, *Phys. Rev. Lett.* **82**, 1406 (1999).
- [27] I. Bouchoule et al., *Phys. Rev. A* **59**, R8 (1999); M. Morinaga, I. Bouchoule, J.-C. Karam, and C. Salomon, *Phys. Rev. Lett.* **83**, 4037 (1999).
- [28] I. Bouchoule, Ph.D. thesis, LKB ENS, Paris, 2000; I. Bouchoule, M. Morinaga, C. Salomon, and D. S. Petrov, *Phys. Rev. A* **65**, 033402 (2002).
- [29] A. A. Abrikosov, L. P. Gorkov, and I. E. Dzyaloshinski, *Methods of Quantum Field Theory in Statistical Physics* (Gover Publications Inc., New York, 1975).
- [30] E. P. Gross, *Nuovo Cimento* **20**, 454 (1961); *J. Math. Phys.* **4**, 195 (1961).
- [31] L. P. Pitaevskii, *Sov. Phys. JETP* **13**, 451 (1961).
- [32] E. M. Lifshitz and L. P. Pitaevskii, *Statistical Physics, Part 2* (Pergamon Press, Oxford, 1980).
- [33] P. G. de Gennes, *Superconductivity of Metals and Alloys* (Benjamin, New York, 1966).
- [34] S. T. Beliaev, *Sov. Phys. JETP* **34**, 323 (1958).
- [35] Yu. Kagan et al., *Phys. Rev. A* **61**, 043608 (2000).
- [36] S. Stringari, *Phys. Rev. Lett.* **77**, 2360 (1996).
- [37] P. Ohberg et al., *Phys. Rev. A* **56**, R3346 (1997).
- [38] M. Flieser, A. Cordas, P. Szepfalussy, and R. Graham, *Phys. Rev. A* **56**, R2533 (1997).
- [39] F. Dalfovo, S. Giorgini, L. P. Pitaevskii, and S. Stringari, *Rev. Mod. Phys.* **71**, 463 (1999).
- [40] S. Stringari, *Phys. Rev. A* **58**, 2385 (1998).
- [41] T.-L. Ho and M. Ma, *J. Low Temp. Phys.* **115**, 61 (1999).
- [42] M. D. Girardeau, *J. Math. Phys.* **1**, 516 (1960); *Phys. Rev.* **139**, B500 (1965).
- [43] E. H. Lieb and W. Liniger, *Phys. Rev.* **130**, 1605 (1963); E. H. Lieb, *ibid*, **130**, 1616 (1963).

- [44] L. Tonks, Phys. Rev. 50, 955 (1936).
- [45] C. N. Yang and C. P. Yang, J. Math. Phys. 10, 1115 (1969).
- [46] L. Reatto and G. V. Chester, Phys. Rev. 155, 88 (1967).
- [47] M. Schwartz, Phys. Rev. B 15, 1399 (1977).
- [48] F. D. M. Haldane, Phys. Rev. Lett. 47, 1840 (1981).
- [49] L. P. Pitaevskii and S. Stringari, J. Low Temp. Phys. 85, 377 (1991).
- [50] D. J. Scalapino, M. Sears, and R. A. Ferrell, Phys. Rev. B 6, 3409 (1972).
- [51] Y. Castin et al., J. Mod. Opt. 47, 2671 (2000).
- [52] C. Mora and Y. Castin, Phys. Rev. A 67, 053615 (2003).
- [53] D. L. Luxdat and A. Gri n, Phys. Rev. A 67, 043603 (2003).
- [54] F. Schreck et al., Phys. Rev. Lett. 87, 080403 (2001).
- [55] M. Greiner et al., Phys. Rev. Lett. 87, 160405 (2001).
- [56] M. Olshanii, Phys. Rev. Lett. 81, 938 (1998).
- [57] D. S. Petrov, G. V. Shlyapnikov, and J. T. M. Walraven, Phys. Rev. Lett. 85, 3745 (2000).
- [58] E. W. Hagley et al., Science 283, 1706 (1999).
- [59] I. Bloch, T. W. Hansch, and T. Esslinger, Nature (London) 403, 166 (2000).
- [60] D. S. Petrov, G. V. Shlyapnikov, and J. T. M. Walraven, Phys. Rev. Lett. 87, 050404 (2001).
- [61] S. Dettmer et al., Phys. Rev. Lett. 87, 160406 (2001).
- [62] D. Hellweg et al., Appl. Phys. B 73, 781 (2001).
- [63] S. Richard et al., Phys. Rev. Lett. 91, 010405 (2003).
- [64] F. Gebier et al., Phys. Rev. A 67, 051602 (2003).
- [65] D. Hellweg et al., Phys. Rev. Lett. 91, 010406 (2003).
- [66] I. Shvachuk et al., Phys. Rev. Lett. 87, 160406 (2002).
- [67] H. Moritz et al., Phys. Rev. Lett. 91, 250402 (2003).
- [68] B. Laburthe Tolra et al., Phys. Rev. Lett. 92, 190401 (2004).
- [69] M. A. Cazalilla, Journal of Physics B: At. Opt. Phys. 32, S1 (2004).
- [70] D. M. Gangardt and G. V. Shlyapnikov, Phys. Rev. Lett. 90, 010401 (2003).
- [71] D. C. Mattis, The Many Body Problem: An Encyclopedia of Exactly Solved Models in 1D (World Scientific, 1994).
- [72] M. M ehta, Random Matrices (Academic, Boston, 1991), 2nd ed.
- [73] V. E. Korepin, N. M. Bogoliubov and A. G. Izergin, Quantum Inverse Scattering Method and Correlation Functions, (Cambridge University Press 1993).
- [74] A. Lenard, J. Math. Phys. 5, 930 (1964); J. Math. Phys. 7, 1268 (1966).
- [75] H. G. Vaidya and C. A. Tracy, Phys. Rev. Lett. 42, 3 (1979); J. Math. Phys. 20, 2291 (1979).
- [76] M. Jimbo and T. Miwa, Phys. Rev. D 24, 3169 (1981).
- [77] V. E. Korepin, Comm. Math. Phys. 94, 93 (1984).
- [78] D. B. Creamer, H. B. Thacker and D. W. Wilkinson, Physica D 20, 155 (1986).
- [79] K. V. Khachatryan, D. M. Gangardt, P. D. Drummond, and G. V. Shlyapnikov, Phys. Rev. Lett. 91, 040403 (2003).
- [80] D. M. Gangardt and G. V. Shlyapnikov, New Journal of Physics, 5, 79 (2003).
- [81] V. Dunjko, V. Lorent, and M. Olshanii, Phys. Rev. Lett. 86, 5413 (2001).
- [82] C. Menotti, private communication.
- [83] C. Menotti and S. Stringari, Phys. Rev. A 66, 043610 (2002).
- [84] R. Combescot and X. Leyronas, Phys. Rev. Lett. 89, 190405 (2002).
- [85] P. J. Forrester, N. E. Frankel, T. M. Garoni and N. S. Witte, Phys. Rev. A 67, 043607 (2003).
- [86] Yu. Kagan, B. V. Svistunov, and G. V. Shlyapnikov, JETP Letters 42, 209 (1985); *ibid* 48, 56 (1988).
- [87] G. E. Astrakharchik and S. Giorgini, Phys. Rev. A 68, 031602 (2003).
- [88] H. Hellmann, Z. Physik. 85, 180 (1933);
- [89] R. P. Feynman, Phys. Rev. 56, 340 (1939).
- [90] R. M. Zi, G. E. Uhlenbeck, and M. Kac, Phys. Rep. 32, 169 (1977).